UNIVERZITA KARLOVA
Přírodovědecká fakulta
Katedra parazitologie

Studijní program: Biologie
Studijní obor: Parazitologie

Bc. Ronald Malych

Proteins interacting with oxygen and its reactive species in *Naegleria gruberi*

Proteiny interagující s kyslíkem a jeho reaktivními formami u *Naegleria gruberi*

DIPLOMOVÁ PRÁCE

Školitel: RNDr. Róbert Šuťák, Ph.D.
Konzultant: doc. RNDr. Ivan Hrdý, Ph.D.

Praha 2020

Prohlášení

Prohlašuji, že jsem závěrečnou práci zpracoval samostatně a že jsem uvedl všechny použité informační zdroje a literaturu. Tato práce ani její podstatná část nebyla předložena k získání jiného nebo stejného akademického titulu.

V Praze dne ……..……..

Poděkování

Rád bych poděkoval svému školiteli RNDr. Róbertu Šuťákovi, Ph.D. a konzultantovi doc. RNDr. Ivanovi Hrdému, Ph.D. za jejich ochotu, vstřícnost a rady při práci v laboratoři a během psaní této práce. Dále chci poděkovat celému kolektivu laboratoře, který se zasloužil o mnoho příjemných zážitků a díky, kterému byla práce zábavou. Nakonec bych rád poděkoval svojí rodině, přítelkyni a všem přátelům za jejich podporu.

Abstrakt

Naegleria gruberi je volně žijící nepatogenní améba. Je to blízký příbuzný patogenní *Naegleria fowleri*, která způsobuje primární amébovou meningoencefalitidu u lidí (PAM). Jako volně žijící organismus je *Naegleria gruberi* přizpůsobena aerobnímu způsobu života, ale má také některé pozoruhodné rysy anaerobního organismu, jako je např. přítomnost Fe-Fe hydrogenázy, která je schopná produkce vodíku.

Tato práce se zaměřuje na tři typy železo obsahujících proteinů, interagujících s kyslíkem a jeho reaktivními formami (ROS), které byly odhaleny v genomu *N. gruberi* - hemerythrin, protoglobin a rubrerythrin. Studované proteiny byly izolovány a purifikovány jako rekombinantní proteiny, proti kterým byly vytvořeny protilátky. V genomu *N. gruberi* nalezený jediný homolog rubrerythrinu jsme úspěšně lokalizovali v mitochondrii, na rozdíl od hemerythrinu a protoglobinu, které vykazují cytosolickou lokalizaci. Charakterizace těchto rekombinantních proteinů *in vitro* zahrnovala hlavně chromatografii na molekulárních sítech a UV-vis spektrofotometrii. Schopnost vázat kyslík byla prokázána spektrálními změnami rekombinantního hemerythrinu, purifikovaného za anaerobních podmínek, a rekombinantního protoglobinu, izolovaného aerobně. Analýza western blot odhalila změny exprese těchto proteinů v *N. gruberi* kultivovaných se sloučeninami produkujícími ROS nebo při kultivaci s různými koncentracemi mědi a železa. Naše výsledky ukazují na roli těchto proteinů v ochraně proti oxidačnímu stresu a / nebo v homeostáze kovů, což obojí jsou rozhodující mechanismy pro přežití buněk.

Abstract

Naegleria gruberi is a free-living non-pathogenic amoeba. It is a close relative to *Naegleria fowleri*, a pathogen that causes primary amoebic meningoencephalitis in humans (PAM). As a free-living organism, *Naegleria gruberi* is adapted to aerobic lifestyle but also possesses remarkable traits of anaerobic organism such as Fe-Fe hydrogenase capable of hydrogen production.

This work focuses on three types of iron-containing proteins interacting with oxygen and its reactive species (ROS) that were uncovered in the genome of *N. gruberi* - hemerythrin, protoglobin and rubrerythrin. Studied proteins have been isolated and purified as recombinant proteins and antibodies have been produced against all three of them. We found a single homolog of rubrerythrin in the genome of *N. gruberi* and successfully localised it in the mitochondrion in contrast to hemerythrin and protoglobin that exhibit cytosolic localisation. *In vitro* characterization of these recombinant proteins included mainly size-exclusion chromatography and UV-vis spectrophotometry. Ability to bind oxygen was shown by spectral changes of recombinant hemerythrin purified under anaerobic conditions and recombinant protoglobin isolated aerobically. Western blot analysis revealed changes in expression levels of these proteins in *N. gruberi* cultivated with ROS-inducing compounds or under conditions of different copper and iron concentrations. Our results indicate the role of these proteins in the protection against oxidative stress and/or in the homeostasis of metals which are mechanisms crucial for cell survival.

1 Introduction

Naegleria spp. is a genus of free-living amoebas capable of transformation to flagellate forms. The most notable representative of this genus is *Naegleria fowleri*, a human pathogen that causes deadly disease, primary amoebic meningoencephalitis (PAM). Close relative and the model for safe studying of *Naegleria* is *Naegleria gruberi*. The sequenced genome of *N. gruberi* unveiled its diverse metabolic features and potential capability to live in both aerobic and anaerobic environment.

Hemerythrin proteins are a group of proteins that contain di-iron centre capable of oxygen-binding. Their function has been described as O_2 transporters in marine invertebrates circulatory system and muscles. New studies report that hemerythrin and hemerythrin-domain may play role in defence against reactive oxygen species, repair of iron-sulfur clusters or be part of iron regulation machinery.

Protoglobin is a hem-containing protein that is part of globin family. It was described as ancestral protein of this family as it was first described in methanogenic archaea. Studies of this protein showed its capability of binding O_2, CO and NO reversibly *in vitro* but its biological role remains unknown.

Rubrerythrin is a di-iron centre containing protein involved in oxidative stress tolerance, functioning as peroxide scavenger in anaerobic bacteria. The protein consists of two parts, the N-terminal di-iron centre containing part that is described to participate in the reduction of hydrogen peroxide, and the C-terminal domain related to the rubredoxin family proteins that is responsible for electron transfer during the peroxide reduction.

All three proteins are present in the genome of *N. gruberi* and represent the subject of the thesis.

2 Review of literature

2.1 *Naegleria* spp.

The first reference of amoeba that could transform into flagellate comes from 19th century (Schardinger, 1899). Research on *Naegleria* spp. has been focused primarily on the mechanism of transformation into flagellate (Fulton & Dingle, 1967) (whole life cycle of *Naegleria* is depicted in Figure 1) until first cases of fatal brain infection, primary amoebic meningoencephalitis in humans, were discovered to be caused by *Naegleria* spp., named *Naegleria fowleri* (Carter, 1970). Although infections are rare, the mortality due to this disease is extremely high. Beside this human pathogen two other species non-pathogenic for humans, *Naegleria australiensis* and *Naegleria italica*, are capable of infection in experimental animals (de Jonckheere et al., 1984). Till now, 47 different species of genus *Naegleria* have been described all over the world (de Jonckheere, 2014), even in Arctic and sub-Antarctic regions (de Jonckheere, 2006).

The model organism for safe studying of *Naegleria* is *Naegleria gruberi*. The model was established for its easy cultivation, non-pathogenicity, as well as its sequenced genome (Fritz-Laylin et al., 2010; Fulton et al., 1984). *N. gruberi* in contrast to *Naegleria fowleri,* cannot survive temperatures higher than 37 °C which can be the reason why *Naegleria gruberi* is non-pathogenic (Griffin, 1972). The recently sequenced genome of another non-pathogenic species *Naegleria lovaniensis* uncovers its close relation to *Naegleria fowleri* and can help in identifying virulence factors of *Naegleria fowleri* (Liechti et al., 2018).

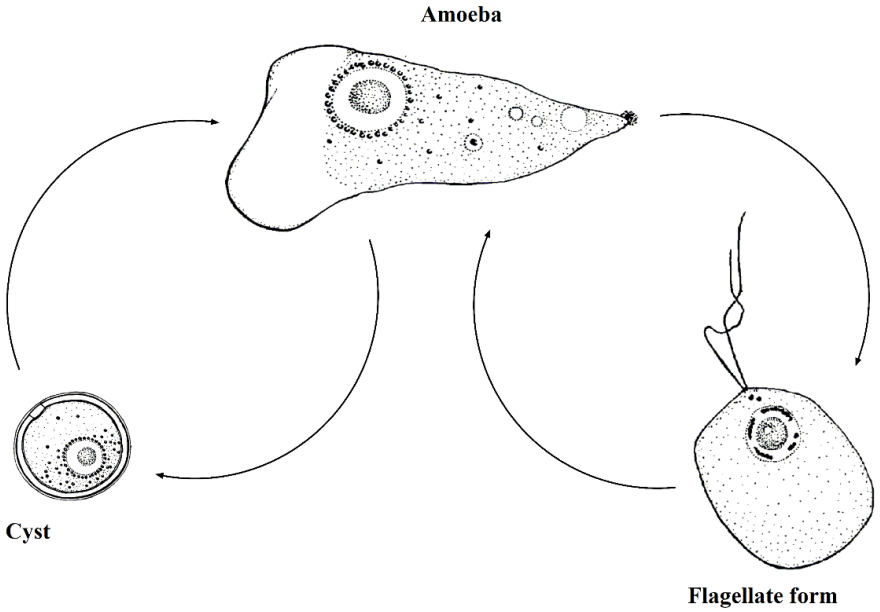

Figure 1. The life cycle of *Naegleria gruberi* with transformations between cyst form, amoeboid trophozoite and flagellate form with two flagella. Figure modified from (Page, 1967).

2.1.1 Metabolism of *Naegleria gruberi*

Naegleria gruberi inhabits environments rich in organic matter (soil, mud), freshwater habitats (rivers, lakes) or swamps. In nature, this organism is a phagotroph feeding on bacteria, but it can be cultured on axenic medium with no bacterial food source (Fulton, 1970).

The sequenced genome unveiled interesting metabolic features with potential capability of life in anaerobic environment (Fritz-Laylin et al., 2010). The main energy-conserving metabolic pathways in *Naegleria gruberi* consist of glycolysis, amino acid catabolism and β-oxidation of fatty acids. Products of these reactions are used in mitochondria, where they are oxidised via Krebs cycle and mitochondrial respiratory chain using oxygen as a terminal electron acceptor. *Naegleria gruberi* also possesses one of the key features of anaerobic metabolism: Fe-Fe hydrogenase and its related maturases (Fritz-Laylin et al., 2011). Predicted mitochondrial targeting signals suggested that this enzyme is localised inside the mitochondrion. However, study of *Naegleria gruberi* Fe-Fe hydrogenase localised this enzyme into cytosol (Tsaousis et al., 2014).

Naegleria gruberi has a complete set of enzymes for the glycolytic pathway with minor changes compared to other eukaryotes. It uses glucokinase and pyrophosphate-dependent phosphofructokinase in the first two phosphorylation steps of glycolysis. The cell also contains pyruvate-phosphate dikinase responsible for the conversion of phosphoenolpyruvate to pyruvate (Opperdoes et al., 2011).

Mitochondrion of *Naegleria gruberi* contains 49833 bp genome encoding 69 genes. It has a fully functional electron transport chain with four protein complexes, capable of electron transport coupled with the transfer of protons and possesses F_1F_O-type ATPase utilizing proton gradient in the production of ATP. Genomic data also revealed some unusual enzymes inside *Naegleria* mitochondrion, particularly three homologs of plant-like alternative oxidase (AOX) and alternative NADH dehydrogenase (NDH2) (Fritz-Laylin et al., 2010; Opperdoes et al., 2011). Alternative oxidase is a membrane protein capable of reduction of O_2 to H_2O without the transfer of protons through the inner mitochondrial membrane (Vanlerberghe, 2013). This enzyme is not unusual for protists as it can be found in *Trypanosoma brucei* (Chaudhuri et al., 1998) or *Cryptosporidium parvum* (Suzuki et al., 2004).

Fatty acids are important organic molecules that can be found in living organisms in different forms. They can serve as a source of energy or be a structural component of cells. *Naegleria gruberi* feeds on bacteria through phagocytosis and degrades their lipid membranes rich in fatty acids. For this degradation, *Naegleria* uses the whole set of phospholipases and lipases for the hydrolysis of triglycerides to glycerol and fatty acids. Free fatty acids are further degraded by β-oxidation inside mitochondrion and predicted peroxisomes (several homologs of proteins participating in the biogenesis of peroxisomes, called peroxins, have been identified in *Naegleria gruberi*) (Opperdoes et al., 2011). From a number of experiments, it was shown that lipids are the preferred growth substrate for *Naegleria gruberi* (Bexkens et al., 2018).

Naegleria gruberi is also able to fully catabolise all proteinogenic amino acids that may serve as an alternative energy source in the absence of lipids and carbohydrates. On the other hand, the cell is not able to synthesise branched and aromatic amino acids that have to be supplemented in the medium for growth in axenic culture (Fulton et al., 1984). The whole predicted metabolic pathway can be seen in Figure 2, page 5.

Iron is an essential nutrient for the stable function of cells. It is a cofactor for proteins involved in energy metabolism, photosynthesis or a cofactor of proteins involved in oxygen transport. Therefore, the homeostasis of this metal is crucial for all forms of life. Not surprisingly, *Naegleria gruberi* genome contains a whole range of iron-containing enzymes and proteins such as fumarase, aconitase, ribonucleotide reductase, lipoyl synthase and many others including Fe-Fe hydrogenase. *Naegleria gruberi* also has a single gene for mitochondrial ferritin that is proposed to function as an iron manager, providing iron to proteins inside mitochondrion (Mach et al., 2018).

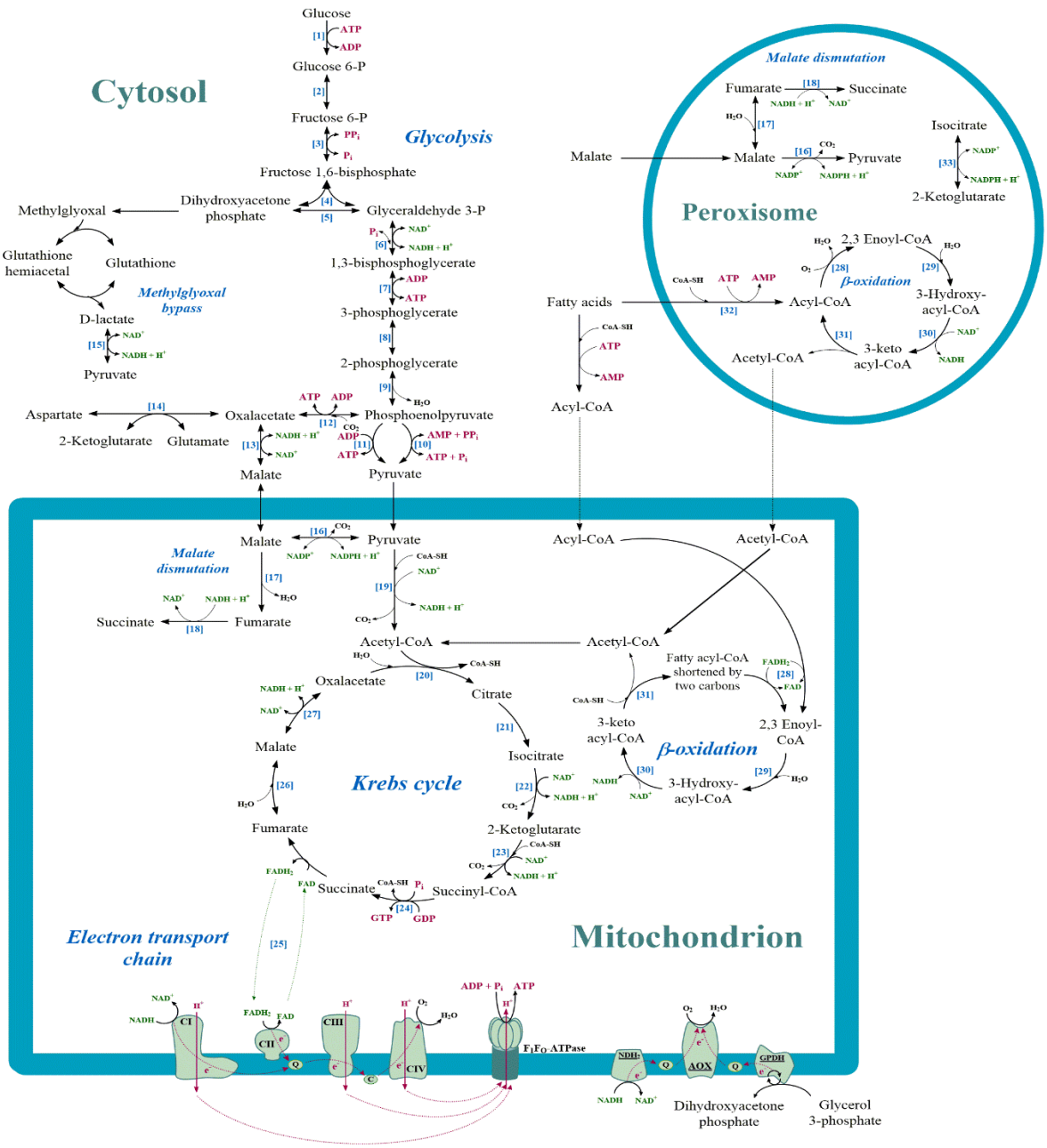

Figure 2. Predicted pathways of energy metabolism in *Naegleria gruberi*. Enzymes: [1] glucokinase, [2] phosphoglucose isomerase, [3] PPi-dependent phosphofructokinase, [4] fructose-bisphosphate aldolase, [5] triosephosphate isomerase, [6] glyceraldehyde-3-phosphate dehydrogenase, [7] phosphoglycerate kinase, [8] phosphoglycerate mutase, [9] enolase, [10] pyruvate phosphate dikinase, [11] pyruvate kinase, [12] phosphoenolpyruvate carboxykinase, [13] malate dehydrogenase (cytosolic), [14] aspartate aminotransferase, [15] D -lactate dehydrogenase, [16] malic enzyme, [17] fumarate hydratase, [18] NADH-dependent fumarate reductase, [19] pyruvate dehydrogenase complex, [20] citrate synthase, [21] aconitase, [22] isocitrate dehydrogenase, [23] 2-ketoglutarate dehydrogenase, [24] succinyl-CoA synthetase, [25] succinate dehydrogenase, [26] fumarate hydratase, [27] malate dehydrogenase, [28] acyl-CoA dehydrogenase, [29] enoyl-CoA hydratase, [30] 3-hydroxyacyl-CoA dehydrogenase, [31] thiolase, [32] Acyl-CoA synthetase, [33] isocitrate dehydrogenase. Electron transport chain proteins: [CI] NADH:ubiquinone oxidoreductase, [CII]

succinate dehydrogenase, [CIII] coenzyme Q:cytochrome c-oxidoreductase, [CIV] cytochrome c oxidase, [NDH2] alternative NADH-ubiquinone oxidoreductase, [AOX] alternative oxidase, [GPDH] glycerol-3-phosphate dehydrogenase. Figure based on predicted metabolic maps in (Bexkens et al., 2018; Opperdoes et al., 2011).

2.2 Oxygen transporting proteins

Molecular oxygen is a vital molecule for the survival of most organisms. For better distribution of O_2 in bodies of multicellular organisms, these organisms use highly soluble proteins evolved to transport O_2. Till today three structurally distinct types of O_2 transporters have been described - hemoglobins, hemocyanins and hemerythrins. Hemoglobin and hemerythrin utilize iron as the prosthetic group able to reversibly bind O_2, unlike hemocyanin that uses copper. In hemoglobin protein family O_2 binds to heme (Fe(II) porphyrin). These proteins can be found in bacteria, plants, invertebrates and vertebrates. The active O_2 binding site in hemocyanin contains a pair of copper atoms. It is a typical dioxygen carrier for invertebrates (octopus, snail, etc.). The last family of O_2 transporters is the hemerythrin family. Their occurrence is rare in comparison to the other two families. Their O_2 binding site consists of two iron atoms (Bertini et al., 2007; Weber & Vinogradov, 2001).

2.3 Hemerythrin

Hemerythrins were first described in three phyla of marine invertebrates (Brachiopoda, Priapulida and Annelida) as proteins capable of O_2 transport. However, recent studies show that hemerythrins are not exclusive for marine invertebrates. There are reports of hemerythrin-like proteins from bacteria, archaea, plants and even human (Alvarez-Carreño et al., 2018).

First reports and characterisation of prokaryotic hemerythrins come from anaerobic sulfate-reducing bacterium *Desulfovibrio vulgaris* and methanotrophic bacterium *Methylococcus capsulatus. Desulfovibrio vulgaris* chemotaxis protein, DcrH, contains a C-terminal hemerythrin-like domain able to bind O_2. It was proposed that the role of this protein is to act as an oxygen sensor for aerotaxis (Xiong et al., 2000). Bacteriohemerythrin from *Methylococcus capsulatus* is a monomeric hemerythrin that participates in the process of methanogenesis. Its role rests in the transport of O_2 molecule from the cytoplasm to methane monooxygenase in intracytoplasmic membranes which converts inert methane into more active methanol (Chen et al., 2012).

Recent studies show that the transport of O_2 is not the only function of hemerythrins and hemerythrin-like proteins. RIC protein of *Escherichia coli* plays a role in the repair of iron-sulfur clusters in enzymes aconitase and fumarase. This protein donates one of the irons from its di-iron centre to repair damaged cluster (Justino et al., 2007; Silva et al., 2018). P_{1B}-type ATPase containing hemerythrin-like domain has been identified in gram-positive bacterium *Acidothermus cellulolyticus* and nitrogen-fixing bacterium *Sinorhizobium meliloti*. These ATPases play a role in detoxification of

Fe and Ni, maintaining homeostasis by means of transport and sensing, preventing their accumulation inside the cell (Traverso et al., 2010; Zielazinski et al., 2013).

Hemerythrin-like proteins have also been found in plants where they form two distinct groups. The first group represents hemerythrin domain containing BRUTUS proteins that exhibit E3 ligase activity and play a role in iron regulation (Matthiadis & Long, 2016). The second group is made up of hemerythrin class glutathione S-transferases that contain C-terminal hemerythrin domains. The function of these glutathione transferases is still unknown, but they are predicted to be involved in heavy metal detoxification (Liu et al., 2013).

Human F-box and leucine-rich repeat protein 5 (FBXL5) contains an N-terminal hemerythrin domain that acts as an iron sensor. FBXL5 plays an important role in the regulation and homeostasis of cellular iron metabolism. It mediates the interaction between E3-ubiquitin ligase complex and iron regulatory protein 2 (IRP2), resulting in ubiquitination of IRP2 and its degradation in proteasome (Muto et al., 2017; Salahudeen et al., 2009).

Hemerythrins can exist in many different oligomeric forms, including the simplest monomers to more complex octamers. The structure of the metal centre responsible for oxygen binding consists of two iron atoms bound to protein by side-chain residues of seven amino acids. These iron atoms are connected together by oxygen atom that is believed to be derived from water (Kurt& et al., 1977).

The main function of hemerythrin in marine invertebrates is the binding and release of oxygen. For this type of reaction, two main redox states of the di-iron centre exist. Deoxyhemerythrin is a reduced state with a diferrous binding site. After binding with the O_2 molecule, the differrous metal centre is oxidized to diferric which forms oxyhemerythrin. A third redox state is formed by autooxidation of oxyhemerythrin after prolonged exposure to O_2. This state is called methemerythrin and it is unable to further react with O_2. Methemerythrin has to be reduced back to deoxyhemerythrin to secure further reactions with O_2 (Howard & Reest, 1991). The whole redox cycle is shown in Figure 3, page 8.

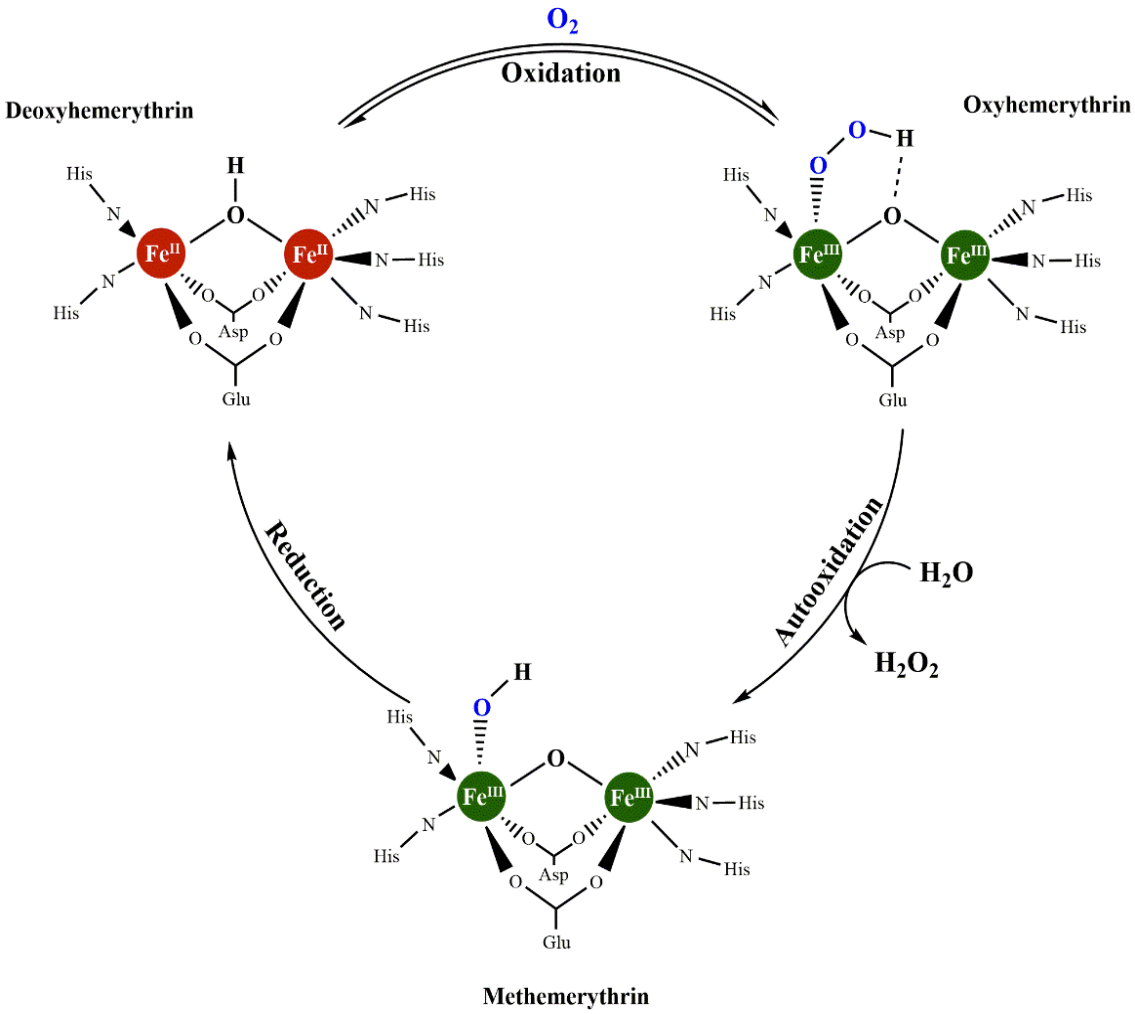

Figure 3. General redox reactions of hemerythrin. Figure shows reduced state of di-iron centre in deoxy form and its oxidation to oxy form. Autooxidation of oxy form to met form is accompanied by the formation of hydrogen peroxide. Based on (Kao et al., 2008).

2.4 Protoglobin

Globins are the most studied family of proteins. Phylogenetic analysis of putative globin sequences revealed the presence of three globin lineages – myoglobin-like globins, sensor globins and truncated globins (Vinogradov, Bailly, et al., 2013). The first lineage, myoglobin-like globins is represented by flavohemoglobins, proteins involved in nitric oxide detoxification. They consist of the C-terminal flavin domain transferring electrons to N-terminal heme containing globin domain (Guanghui Wu et al., 2003). Flavohemoglobins play an important role as protectors against nitrosative stress in pathogenic microorganisms. Their presence within *Salmonella enterica* was shown to help with its survival inside human macrophages (Gilberthorpe et al., 2007). These proteins are not exclusive to bacteria. Human parasite *Giardia intestinalis* contains flavohemoglobin which might play a role in defence of the parasite against NO-mediated human host response (Mastronicola et al., 2010). Pathogenic fungi *Candida albicans* and *Cryptococcus neoformans* also contain flavohemoglobins that are part of nitric oxide detoxification machinery and can promote virulence of these pathogens (Chiranand et al., 2008; de Jesús-Berríos et al., 2003).

The truncated globins are mainly bacterial proteins but can also be found in plants, green algae, diatoms and ciliates. Their size is shorter than oxygen transporting hemoglobins (Vinogradov & Moens, 2008). Proposed functions for truncated globins include protection against reactive oxygen species and reactive nitrogen species, dioxygen scavenging and possible sulfide-binding (Nicoletti et al., 2010; Ouellet et al., 2002; Parrilli et al., 2010).

Globin-coupled sensors are a family of globins functioning primarily as oxygen sensors. These proteins consist of the N-terminal sensor domain with heme and many different types of C-terminal output domains. The most prevalent group of globin-coupled sensors are the ones with methyl accepting chemotaxis protein output domains (Vinogradov, Tinajero-Trejo, et al., 2013). Heme chemotaxis transducer from *Bacillus subtillis* is the best characterised protein of this group that generates an aerophilic response to changing O_2 levels (Hou et al., 2000). Another group of globin-coupled sensors serves as second messengers in bacteria and can play a role in biofilm formation. These proteins contain diguanylate cyclase as their output domain (Burns et al., 2016). A special case of globin with second messenger domain is globin-coupled heme containing adenylate cyclase from *Leishmania major* which produces cAMP that controls gene expression, helping the cell to survive hypoxia (Santara et al., 2013).

Protoglobins are part of sensor globin lineage and they are believed to be ancestors of all sensor globins (Nardini et al., 2008). The most biochemically and functionally characterised protoglobins come from two archaea - obligatory aerobic hyperthermophile *Aeropyrum pernix* and strictly anaerobic methanogen *Methanosarcina acetivoran.* The function of these proteins is still unknown as they do not show specificity for only one type of ligand. Instead, they display wide range of ligand possibilities including binding of molecular oxygen, carbon monoxide and nitric oxide

(Allen Freitas et al., 2004). Figure 4 shows the potential reaction of protoglobin heme with molecular oxygen.

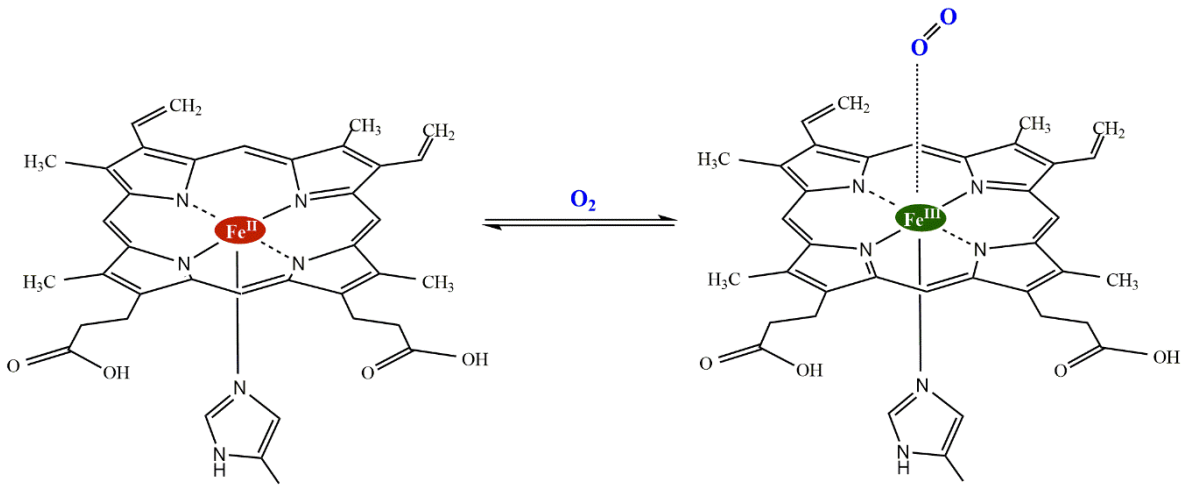

Figure 4. Potential reaction of heme centre in protoglobin with molecular oxygen, analogous to hemoglobin reaction with oxygen. Based on (Bertini et al., 2007).

2.5 Reactive oxygen species

The rise of O_2 levels on primordial Earth played an important role in the evolution of multicellular organisms. The availability of atmospheric O_2 allowed early life forms to produce energy more efficiently that resulted in increase of complexity of organisms (Thannickal, 2009). But using O_2 in metabolic processes within cells has also its price as it results in the production of reactive oxygen species such as superoxide anion ($O_2^{\cdot -}$), hydroxyl ($HO^{\cdot}$), peroxyl ($ROO^{\cdot}$) radical and non-radical hydrogen peroxide (H_2O_2). These molecules are highly reactive and may cause DNA damage, lipid peroxidation and protein oxidation. To combat reactive oxygen species, cells have developed several enzymatic and non-enzymatic protective mechanisms (Apel & Hirt, 2004).

Non-enzymatic protection against reactive oxygen species inside cells is mediated by low molecular weight antioxidants such as ascorbate and glutathione as well as tocopherol, flavonoids and carotenoids in plants (Das & Roychoudhury, 2014). Main enzymatic protection is composed of superoxide dismutase, catalase and glutathione-linked and thioredoxin-linked detoxification systems (Auten & Davis, 2009).

Superoxide dismutase is an enzyme specifically used for superoxide anion detoxification. The mechanism of detoxification lies in the conversion of reactive superoxide anion to hydrogen peroxide (H_2O_2) and molecular oxygen (O_2). Depending on metal cofactor, superoxide dismutases can be divided into four groups: iron-containing (FeSOD) typically found in chloroplasts, manganese-containing (MnSOD) localised in mitochondrion, copper/zinc-containing (Cu/ZnSOD) that can be found in cytosol and nickel-containing (NiSOD) which is mainly bacterial (Abreu & Cabelli, 2010). *Plasmodium falciparum*, the human parasite causing disease malaria, contains FeSOD (Becuwe et

al., 1996) and has been described to be capable of utilizing host Cu/ZnSOD as well (Steven Meshnick, 1989).

Hydrogen peroxide, produced by superoxide dismutase, has to be further detoxified. For this purpose, cells contain specific detoxification enzymes such as catalase. Catalase is a widely distributed, heme-containing enzyme with one of the highest turnovers among enzymes (Sepasi Tehrani & Moosavi-Movahedi, 2018).

Another important reactive oxygen species scavenger is tripeptide glutathione (GSH, composed of amino acids L-γ-glutamate, L-cysteine and glycine) and its related proteins. Hydrogen peroxide is reduced by enzyme glutathione peroxidase to water utilizing two molecules of glutathione as reductants. The formed glutathione disulfide (GSSG) is reduced by NADPH-dependent glutathione reductase back to two molecules of glutathione. The ratio between GSH/GSSG is usually used as an indicator of cellular antioxidant capacity (Guoyao Wu et al., 2004).

Similar to the glutathione reducing system, cells possess another detoxification system dependent on oxidation and reduction of small protein thioredoxin. The reduction of thioredoxin is mediated by the NADH-dependent enzyme, thioredoxin reductase. Thioredoxin and thioredoxin reductase together with thioredoxin peroxidase or peroxiredoxins create another system able to detoxify reactive oxygen species (Mustacich & Powis, 2000; Rhee, 2016).

Parasitic protists possess both of these two systems as protection against reactive oxygen species. Some species also have some interesting additional proteins and systems that have the potential to help them cope with oxidative stress. One of the examples is the homolog of osmotically inducible protein from *Trichomonas vaginalis*. This protein is linked with incomplete glycine decarboxylase complex comprising a system that serves as peroxide scavenger in hydrogenosomes (Nývltová et al., 2016). Another potential detoxification system in parasitic protists comprises bacterial protein rubrerythrin.

2.5 Rubrerythrin

Erythrins/rubrerythrins are proteins belonging to the ferritin-like superfamily. Proteins from this superfamily have various functions in cells ranging from iron storage (ferritin, bacterioferritin), iron detoxification (DNA-binding protein from starved cells (Dps)), ubiquinone biosynthesis (coenzyme Q7, hydroxylase) to radical scavenging (erythrin/rubrerythrin) (Andrews, 2010).

Rubrerythrin has been described as NADH-dependent peroxidase in sulfate-reducing bacterium *Desulfovibrio vulgaris* reducing H_2O_2 to H_2O (mechanism in Figure 6, page 12) (Coulter et al., 1999). The protein mainly consists of two domains, N-terminal domain with di-iron centre, homologous to ferritin and C-terminal domain with mononuclear iron bound to side chains of four cysteines (deMaré et al., 1996). Several types of rubrerythrins are present in both anaerobic and aerobic microorganisms. Classical rubrerythrins with both di-iron and mononuclear iron centre are

predominantly present in obligate anaerobes as well as reverse type rubrerythrins with change between mononuclear iron site (now at the N-terminal site of the protein) and di-iron site (located at the C-terminal part of the protein) (Cardenas et al., 2016). Beside anaerobic rubrerythrins, two aerobic lineages exist, one in cyanobacteria and other in facultative aerobic organisms. These rubrerythrins are lacking the C-terminal domain that bounds mononuclear iron and is predicted to be responsible for electron transport during catalytic reactions of rubrerythrin (Andrews, 2010).

Rubrerythrins are not entirely exclusive for bacteria. These proteins can be found in genomes of some parasitic protists such as *Trichomonas vaginalis*, *Entamoeba histolytica* or *Spironucleus salmonicida* (Stairs et al., 2019). *Trichomonas vaginalis* rubrerythrin was described as hydrogenosomal protein with a function in protection against oxidative stress (Pütz et al., 2005). Similarly, rubrerythrin from anaerobic amoeba *Entamoeba histolytica* plays a role in protection against reactive oxygen species with its peroxidase activity (Cabeza et al., 2015). This protein was shown to be localised to mitosome (Maralikova et al., 2010).

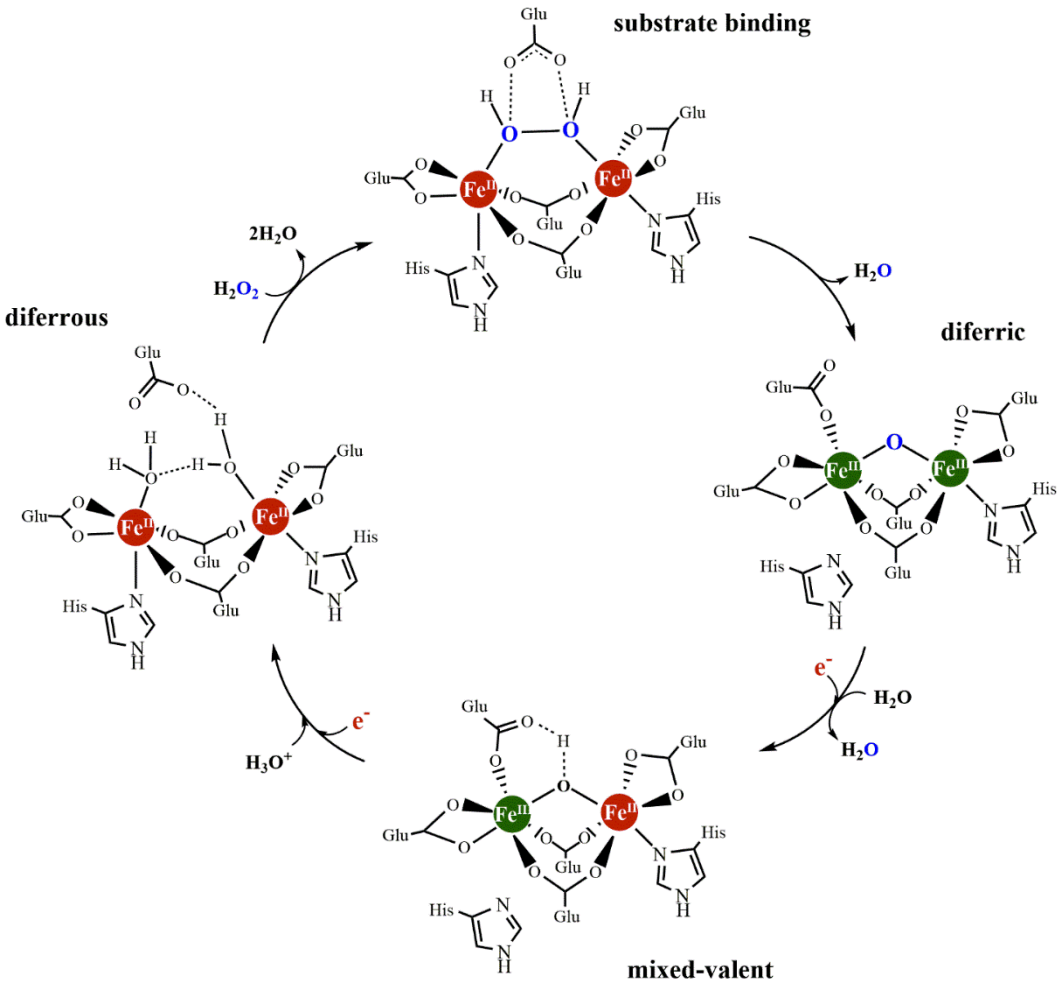

Figure 6. Proposed scheme for peroxidase activity of rubrerythrin. Electron transfer (in red) for reduction of diferric and mixed-valent state are mediated by mononuclear iron at C-terminal domain of rubrerythrin. In blue are oxygen atoms originating from hydrogen peroxide. Based on (Dillard et al., 2011).

3 Aims of the thesis

1. Preparation of *N. gruberi* recombinant proteins hemerythrin, protoglobin and rubrerythrin
2. Preparation of polyclonal antibodies against *N. gruberi* hemerythrin, protoglobin and rubrerythrin
3. Biochemical characterisation of recombinant proteins
4. Localisation of the proteins within *N. gruberi* cell using polyclonal antibodies
5. Studying the effect of different growth conditions on expression levels of the studied proteins using polyclonal antibodies

4 Materials and methods

4.1 Preparation of recombinant proteins

4.1.1 Gene amplification

Plasmid pJET1.2/blunt (Thermo Scientific) with ampicillin resistance for selection was used as a vector for cloning and amplification of genes. Ligation into this plasmid is accomplished by inserting a blunt-ended gene generated by PCR (polymerase chain reaction). Two plasmids were selected for expression of studied *Naegleria gruberi* genes (hemerythrin - XP_002670631.1, protoglobin - XP_002677420.1, rubrerythrin - XP_002682904.1) in *E. coli* - pET42b (Novagen), which allows expression with a C-terminal polyhistidine tag and pET3a (Novagen), used for expression in inclusion bodies. Both plasmids have selective antibiotic resistance (pET42b – kanamycin, pET3a – ampicillin). As one of the targeted genes (rubrerythrin) contains introns, cDNA from *N. gruberi* was used as a template which was provided by RNDr. Jan Mach, Ph.D. For hemerythrin and protoglobin gene whole genomic DNA from *N. gruberi*, isolated using the High Pure PCR Template Preparation Kit (Roche) according to the manufacturer´s protocol, was used as a template for PCR. First, the DNA was amplified using Q5® Hot Start High-Fidelity DNA Polymerase (New England BioLabs) and specific primers for each targeted gene (see Table 1). The reaction mixture and settings for the PCR are shown in Tables 2 and 3.

Table 1. Restriction sites and primers used for amplification of targeted genes into specific plasmids.

Hemerythrin		
pET42b	**Restriction site**	**Primer sequence**
Forward	NdeI	5'- CACCATATGATGTCTTATCCAATCCCAACCCC-3'
Reverse	BamHI	5'- CACGGATCCAATAACACCCTTATACTTCATATCAGAAGC-3'
pET3a	**Restriction site**	**Primer sequence**
Forward	NdeI	5'- CACCATATGATGTCTTATCCAATCCCAACCCC-3'
Reverse	BamHI	5'- CACGGATCCTTAAATAACACCCTTATACTTCATATCAGAAGC-3'
Protoglobin		
pET42b	**Restriction site**	**Primer sequence**
Forward	NdeI	5'-CACCATATGATGCAAACTATCGAAGAAAAGCAAC-3'
Reverse	BamHI	5'-CACGGATCCTTGCTTGTTAGCAAAGATACATCCA-3'
Rubrerythrin		
pET42b	**Restriction site**	**Primer sequence**
Forward	NdeI	5'-ATCCATATGATGTTCAGATCCATCACCAAAGT-3'
Reverse	BamHI	5'-ATCGGATCCTTGAGAAGCTCTTAACTTGTTCA-3'

Table 2. Composition of PCR reaction mixture

Reagent	Volume (µl)
5× Q5 Reaction Buffer	5,00
10 mmol×dm^{-3} dNTPs	0,50
10µM Forward primer	1,25
10µM Reverse primer	1,25
Template DNA	1,00
Q5 DNA Polymerase	0,25
Deionized water	15,75

Table 3. The setting of PCR, number of cycles, temperature and time

Number of cycles	1 x	30 x			1 x	
Temperature	95 °C	95 °C	56 °C	72 °C	72 °C	4 °C
Time (min)	5:00	1:00	1:00	1:00	10:00	∞

4.1.2 Cloning of DNA fragments and transformation into bacteria

The amplified DNA fragments were separated by horizontal gel electrophoresis on a 1 % agarose gel with 0,1 % SYBR safe intercalating dye (Invitrogen). DNA in the gel was visualized using a UV transilluminator and the band of the correct size corresponding to the amplified gene was excised. The next step was the extraction of the excised PCR fragments from the gel using the Gel/PCR DNA Fragments Extraction Kit (Geneaid).

Each amplified gene was inserted into the plasmid pJET1.2/blunt using the CloneJET PCR Cloning kit (Thermo Scientific) according to the manufacturer´s protocol. The resulting plasmid was transformed into competent *E. coli* strain XL1-Blue. Bacteria were preincubated on ice for 30 min with the added vector, followed by a thermal shock at 42 °C for 30 s and re-incubated on ice for 2 min. The last step was the addition 250 µl of preheated SOC medium (Super Optimal Broth with Catabolite Repression, composition in Table 4, page 16) to the cells. The cells were incubated for 1 h at 37 ° C on a shaker at 225 rpm. Finally, cells were plated on a 5 % agarose plate with a selective antibiotic at a final concentration of 100 µg/ml. The plates were incubated overnight in a 37 °C heated thermostat.

Table 4. Composition of SOC medium

Reagent	Mass (g)
Potassium chloride (Sigma)	0,019
Sodium chloride (Sigma)	0,058
Yeast extract (Oxoid)	0,500
Trypton (Oxoid)	2,000
Adjust to pH 7, fill with water up to 100 ml, autoclave	
Glucose (Sigma)	0,360
Magnesium (II) chloride (Sigma)	0,095

After overnight incubation, six bacterial colonies for each gene were picked and transferred into 40 µl of deionized water. A control PCR was performed on these colonies using correct primers for each gene and SapphireAmp Fast PCR Master Mix (Takara) according to the manufacturer´s protocol. After confirming the correct size of the amplified DNA from control PCR, 20 µl of bacteria was transferred into 5 ml LB medium (10 g LB-broth (Sigma) per 500 ml distilled water) with the selective antibiotic. This culture was incubated overnight at 37 °C on a shaker at 225 rpm. Subsequently, plasmid DNA was obtained from the grown cells using a High-Speed Plasmid Mini Kit (Geneaid). The purity and concentration of the obtained plasmid DNA was measured on a NanoDrop 2000 (Thermo Scientific). A sample of the resulting plasmid was also used for sequencing using universal primers against promotor and terminator inside the plasmid to confirm the correct sequence of genes. DNA sequencing was performed by RNDr. Štepánka Hrdá and Mgr. Blanka Hamplová, Ph.D. at OMICS Genomics facility in Biocev.

The next step, after obtaining plasmids with multiplied and correct genes, was to clone these genes into plasmids allowing their expression. Using Thermo Scientific Fast Digest restriction enzyme reaction kit and corresponding restriction enzymes from Table 1, page 14, genes cloned in pJET1.2/blunt plasmid and expression plasmid were digested. The reaction mixture used for restriction is shown in Table 5. The mixture was incubated for 1 h at 37 °C.

Table 5. Reagents for restriction by Thermo Scientific Fast Digest restriction enzymes.

Reagent	Volume (µl)
Plasmid/DNA insert	5,0
10× Fast Digest Green Buffer	1,0
Fast Digest enzyme I	0,5
Fast Digest enzyme II	0,5
Deionised water	3,0

The digested expression plasmid and genes from pJET1.2/blunt plasmid were extracted the same way as PCR fragments (see chapter 4.1.2, page 15). This was followed by a ligation reaction with T4 DNA ligase (Promega). The ligation reaction mixture was mixed according to the manufacturer's protocol and then incubated at 16 °C overnight. The last step was the transformation of ligation mixture into competent *E. coli* strain XL1-Blue. The whole process was the same as described on pages 15 and 16.

Obtained amplified expression plasmid was transformed by heat shock into competent *E. coli* BL21 strain (DE3), which is intended for expression of the recombinant proteins.

4.1.3 Induction of protein expression

To determine the expression level of the proteins in bacteria, 800 µl of pre-grown cells were incubated in 40 ml LB medium until the optical density at 600 nm increased to approximately 0,6. Optical density was measured in 1 cm plastic cuvettes on a WPA CO 8000 Biowave Cell Density Meter (Biochrom). LB medium without bacteria was used as a blank sample. Before the start of protein expression, 800 µl of bacterial culture was centrifuged and boiled in sample buffer (composition in Table 6) as a negative control. IPTG (Isopropyl β-D-1-thiogalactopyranoside (Serva)) was added to the remaining bacterial cultures to a final concentration of 0,5mM, and the cells were incubated for 1 h and 3 h at 37 °C on a shaker at 225 rpm. Samples were taken after the given incubation time and immediately processed in the same manner as a negative control. Expression levels were checked by SDS-PAGE and western blot using a 1:1 000 dilution of primary anti-histidine tag antibody.

After the determination of the level of expression over time from control experiments, selected bacterial colony was grown in 2 l of LB medium without antibiotics and incubated at 37 °C at 225 rpm. After reaching optical density of 0,8, IPTG was added to a final concentration of 0,5mM and culture was incubated for 3 h. After this incubation the grown cells were centrifuged at 3 000 g, 10 min, 4 °C in Avanti J-26 XPI centrifuge (Beckman coulter). The obtained bacterial pellet was washed with 40 ml of phosphate buffer (composition in Table 6) and centrifuged at 3 000 g, 10 min, 4 °C. The washed pellet was used for subsequent purification.

Table 6. Composition of sample buffer and phosphate buffer

Reagent	Volume (ml)
1 M Tris (pH 6,8)	2,4
10 % SDS	2,0
Glycerol	2,5
Deionised water	1,6
0,2 % bromophenol blue	1,0
β-mercaptoethanol	0,5

Reagent	Concentration (mM)
Sodium chloride (Sigma)	137,0
Potassium chloride (Sigma)	2,7
K_2HPO_4 (Lachema)	1,8
NaH_2PO_4 (Sigma)	10,0
pH 7,4	

4.1.4 Isolation of recombinant proteins by affinity chromatography

The bacterial pellet containing the expressed *N. gruberi* protein was resuspended in 20 ml of lysis buffer (composition in Table 7) with added cOmplete EDTA-free protease inhibitor (Roche) according to the protocol. The cells were disintegrated by sonication for 3×60 s at 60 % amplitude (QSonica Q125). The resulting lysate was centrifuged at 200 000 g for 15 min at 4 °C on an Optima XPN-90 Ultracentrifuge (Beckman coulter) with a type 70 Ti rotor. The portion of the resulting pellet was boiled in sample buffer. The supernatant was mixed with 1 ml of HIS-Select Nickel Affinity Gel (Sigma), which selectively binds proteins with polyhistidine tag. This mixture was incubated on a rotator for 1 h at 4 °C. The matrix was captured on a Poly-Prep Chromatography Column (Bio-Rad) and an imidazole concentration gradient was used to release the bound protein from the nickel matrix. The matrix was gradually washed with 3×2 ml of wash buffer, 4×0,5 ml of elution buffer I, 3×0,5 ml of elution buffer II and 3×0,5 ml of elution buffer III (composition in Table 7). Each fraction was collected into a separate tube. An aliquot of every fraction and the matrix itself was boiled in sample buffer and analysed by SDS-PAGE. In the fraction with the largest amount of *N. gruberi* protein, protein concentration was determined using the Bicinchoninic acid kit for protein determination (Sigma).

The entire volume of the fraction most enriched with recombinant protein was boiled in sample buffer and separated on preparative electrophoresis at 250 V. Electrophoresis was stopped when the front of the sample reached the bottom of the gel. The gel was stained overnight with Coomassie Brilliant Blue G-250 then destained in distaining solution (25 % methanol and 10 % acetic acid in distilled water) until the expected protein band was visible. The protein band was carefully excised with a sterile scalpel and washed 3 times with sterile phosphate buffer. A small portion of the gel was sent for proteomic analysis to confirm that it was the correct protein. Analysis was performed by Mgr. Pavel Talacko and Mgr. Karel Harant at OMICS Proteomics facility in Biocev. The last step was a homogenization of the protein band using a Dounce homogenizer (Kimble-chase).

Table 7. Composition of buffers used for isolation of recombinant protein

Lysis buffer	Concentration (mM)	Wash buffer	Concentration (mM)
Sodium chloride (Sigma)	300	**Sodium chloride (Sigma)**	300
Sodium dihydrogen phosphate (Lachner)	50	**Sodium dihydrogen phosphate (Lachner)**	50
Imidazole (Sigma)	10	**Imidazole (Sigma)**	20
pH 8,0		**pH 8,0**	

Elution buffer I	Concentration (mM)
Sodium chloride (Sigma)	300
Sodium dihydrogen phosphate (Lachner)	50
Imidazole (Sigma)	100
pH 8,0	

Elution buffer II	Concentration (mM)
Sodium chloride (Sigma)	300
Sodium dihydrogen phosphate (Lachner)	50
Imidazole (Sigma)	250
pH 8,0	

Elution buffer III	Concentration (mM)
Sodium chloride (Sigma)	300
Sodium dihydrogen phosphate (Lachner)	50
Imidazole (Sigma)	400
pH 8,0	

4.1.5 Immunization of rat

The prepared homogenized protein suspensions were used to rise specific polyclonal antibodies in rats. Before immunization, blood serum from experimental animals was tested for potential antibodies against *N. gruberi*. Whole-cell lysates of *N. gruberi* were analysed by SDS-PAGE and western blot using a serum of experimental animals as the primary antibody. After this control experimental animals were immunized 3 times with 250 µg of protein every 30 days. After the third immunization, a control sample of the serum was taken. When the control showed positive results on western blot the rest of the blood was taken from the rat. Work with experimental animals and their handling was performed by RNDr. Jan Mach, Ph.D.

The collected blood was centrifuged at 2 000 g for 15 min at room temperature. The supernatant was collected and centrifuged again under the same conditions. Resulting antisera were used in further experiments.

4.1.6 Preparation of whole-cell lysates

Cultivation of *N. gruberi* cells is described in chapter 4.4.1, page 27. Cells were collected from culture flasks by shaking, transferred to centrifuge tubes and centrifuged for 10 min, 1 200 g, 4 °C. The resulting pellet of cells was washed twice with sterile phosphate buffer. To ensure even distribution of loaded proteins, the protein concentration was determined by Bicinchoninic acid kit for protein determination (Sigma). At the end pellets were boiled in sample buffer (composition in Table 6, page 17) for 5 min at 100 °C. Whole-cell lysates prepared this way were analysed by SDS-PAGE and western blot using rat polyclonal antibodies against selected *N. gruberi* proteins (see chapter 4.1, page 14).

4.1.7 SDS-PAGE

SDS-PAGE is an electrophoretic method used for the separation of proteins utilising polyacrylamide gels and sodium dodecyl sulfate. Unless stated otherwise, 20 µg of total proteins per sample were used for all analyses. Depending on the size of the protein of interest 12 % to 15 % polyacrylamide gels were used for electrophoresis. Page Ruler Plus Prestained Protein Ladder (Thermo Scientific) was used as a standard for protein size determination. The electrophoresis was carried out at a constant voltage of 150 V for about 90 min.

For visualization, polyacrylamide gels were stained for 1 h by Coomassie Brilliant Blue G-250 (Sigma) and destained with the destaining solution (25 % methanol and 10 % acetic acid (Lachner) in distilled water) until proteins were visible on the gel.

4.1.8 Western blot

For detection of a specific protein in a mixture of proteins, electroblotting to nitrocellulose membrane and its subsequent immuno-detection was used. Proteins separated by SDS-PAGE were transferred from polyacrylamide gel to nitrocellulose membrane by semi-dry transfer. The semi-dry electro-blotting system Fastblot B33 (Biometra) was used for transfer. The transfer was carried out for 75 min at a setting of 1,5 mA/cm^2 of the membrane. After the transmission was complete, the membrane was stained in Ponceau S solution (0,5 % Ponceau S (Merck), 1 % acetic acid (Lachner)) for visualization of proteins.

To prevent non-specific antibody binding, the membrane was incubated in blocking solution (5 % low fat milk and 0,25 % TWEEN20 (Sigma) in phosphate buffer (composition in Table 6, page 17) at 4 °C, overnight. After blocking, the membrane was incubated with the chosen polyclonal antibody for 1 hour at room temperature in blocking solution. After incubation with the primary antibody, the membrane was washed 3x15 min with blocking solution. The next step was the addition of specific secondary antibody conjugated with horseradish peroxidase (Sigma) at a 1:5 000 dilution in blocking solution and subsequent incubation for 1 hour at room temperature.

After washing of the membrane 2x15 min with blocking solution and 1x15 min with phosphate buffer, the nitrocellulose membrane was visualised by chemiluminescence in an Amersham Imager 600 (GE Healthcare) using a commercial peroxidase chemiluminescent substrate Chemiluminescent Peroxidase Substrate 1 (Sigma) according to manufacturer´s protocol.

4.2 Protein characterization

4.2.1 Isolation under native conditions

Recombinant proteins in native conditions were prepared and isolated by affinity chromatography (for the whole process see chapter 4.1.4, page 18). The fraction containing the largest amount of recombinant protein was used for experiments. Proteins isolated by this method contained polyhistidine tag at C-terminus of the protein. For isolation of non-tagged protein, the gene for *N. gruberi* hemerythrin was cloned to plasmid pET3a in the same manner as described in chapters 4.1.1 and 4.1.2, page 14 and 15 and isolated from inclusion bodies (see chapter 4.2.2).

4.2.2 Isolation from inclusion bodies

E. coli BL21 strain (DE3) containing plasmid pET3a with *N. gruberi* hemerythrin gene was grown in 2 l of LB medium. The protein expression was induced in the same manner as described in chapter 4.1.3, page 17. The resulting bacterial pellet was sonicated in lysis buffer (composition in Table 8) for 3×20 s at 60 % amplitude. After sonication, lysate was centrifuged for 20 min at 20 000 g, 4 °C. The pellet, containing inclusion bodies, was washed twice with wash buffer (composition in Table 8). An aliquot of supernatant after sonication, both washes and pellet after washing were boiled in sample buffer and analysed by SDS-PAGE. The washed pellet was resuspended in 20 ml of 6 M guanidine hydrochloride with added β-mercaptoethanol (volume ratio between guanidine hydrochloride and β-mercaptoethanol was 6 ml/100 µl). Pellet was let to dissolve for 3 h at 37 °C. After incubation, suspension was centrifuged for 20 min at 20 000 g, 4 °C. Aliquots of pellet and supernatant were taken for further SDS-PAGE analysis. The rest of the supernatant was dialyzed overnight in SERVAPOR® dialysis tubing against a 1 000x volume of deoxygenated (purged with nitrogen) dialysis buffer (20mM Tris-HCL (Sigma), 150mM NaCl (Sigma), pH 7,4) in the presence of 0,1 g of ferrous ammonium sulfate (Sigma) at 4 °C. Dialyzed protein solution was centrifuged for 20 min at 20 000 g, 4 °C. The precipitate, incurred during dialysis, was boiled in sample buffer and the supernatant was concentrated with Amicon Ultra-4 centrifugal filter unit (Merck) with 3 000 Da molecular weight cut-off membrane, according to the manufacturer´s protocol. An aliquot of both flow-through and concentrated reconstituted protein was boiled in sample buffer and analysed by SDS-PAGE. Reconstituted protein was further used in the spectrophotometric analysis (see chapter 4.2.4, page 24).

Table 8. Composition of buffers for isolation from inclusion bodies

Lysis buffer	Concentration (mM)
Tris (Sigma)	20
Sodium chloride (Sigma)	20
pH 8,0	

Wash buffer	Concentration
Tris (Sigma)	20mM
Urea (Sigma)	2M
TWEEN20 (Sigma)	2 %
pH 8,6	

4.2.3 Size-exclusion chromatography

The first method used for protein characterization was size-exclusion chromatography. Work on liquid chromatograph FPLC Biologic Duo Flow (Bio-Rad) with UV detector (280 nm) and QuadTec detector (four selected wavelengths in visible spectrum) was performed by doc. RNDr. Ivan Hrdý, Ph.D. using software interface Biologic Duo Flow system (Bio-Rad). For analysis of our proteins we used three different columns. For smaller, recombinant *N. gruberi* hemerythrin we used ENrich SEC 70 10/300 column (Bio-Rad). For recombinant *N. gruberi* rubrerythrin we used Superdex 75 Increase 10/300 column (GE Healthcare). Both of these columns have separation range of 500 to 70 000 Da. For larger, recombinant *N. gruberi* protoglobin we used Superdex 200 Increase 10/300 GL column (GE Healthcare) with separation range of 10 000 to 600 000 Da. Recombinant proteins were produced in bacteria and isolated by affinity chromatography (see chapters 4.1.3 and 4.1.4, page 17 and 18). The fraction most enriched with recombinant protein was used for the analysis. Proteins were concentrated by Amicon Ultra-4 Centrifugal Filter Unit (Merck) into the same buffer that was used for liquid chromatography (10mM HEPES (Sigma), 150mM NaCl (Sigma), pH 7,5). 500 µl samples were loaded onto the column, the flow rate was set to 0,75 ml/min and 0,5 ml elution fractions were collected from the fourth min of the chromatography run. For determination of molecular weight of eluted proteins, Gel filtration standard (Bio-Rad) mixture was used (composition in Table 9). The calibration curves for each column (Figure 7, 8 and 9) show the molecular weight standards plotted against their elution time.

Table 9. Composition of Gel filtration standard (Bio-Rad) mixture

Component	Molecular weight (Da)
Thyroglobulin (bovine)	670 000
γ-globulin (bovine)	158 000
Ovalbumin (chicken)	44 000
Myoglobin (horse)	17 000
Vitamin B12	1 350

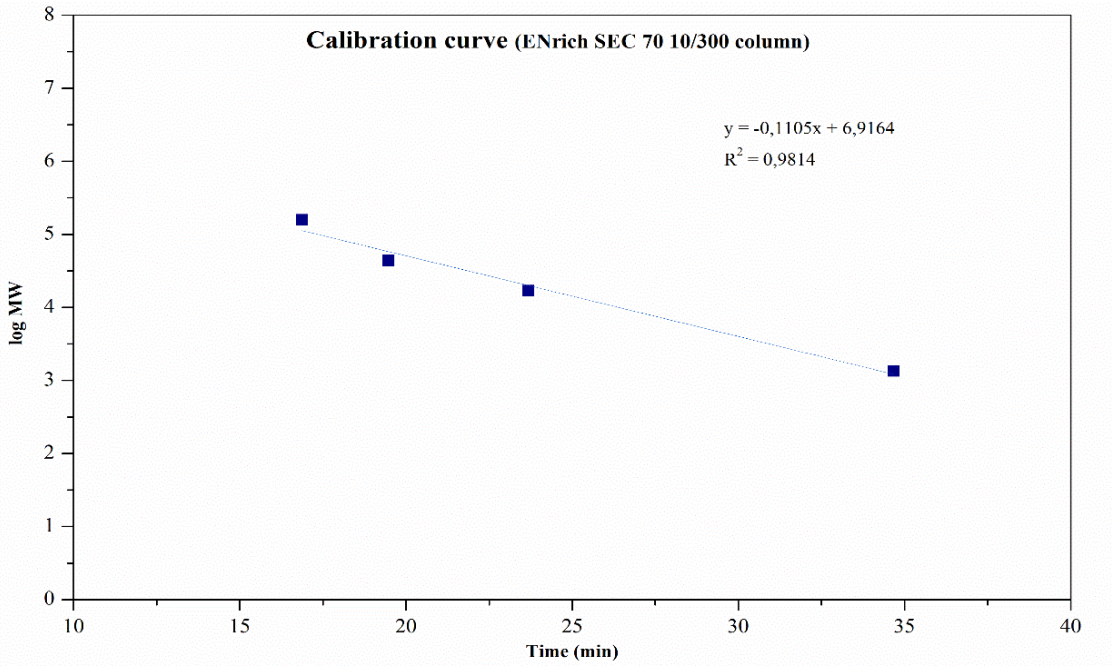

Figure 7 – Calibration curve of Gel filtration standards (Bio-Rad) used for size-exclusion chromatography on ENrich SEC 70 10/300 column (Bio-Rad). Molecular weight in logarithmic scale is on y-axis, elution time of each protein standard is on x-axis.

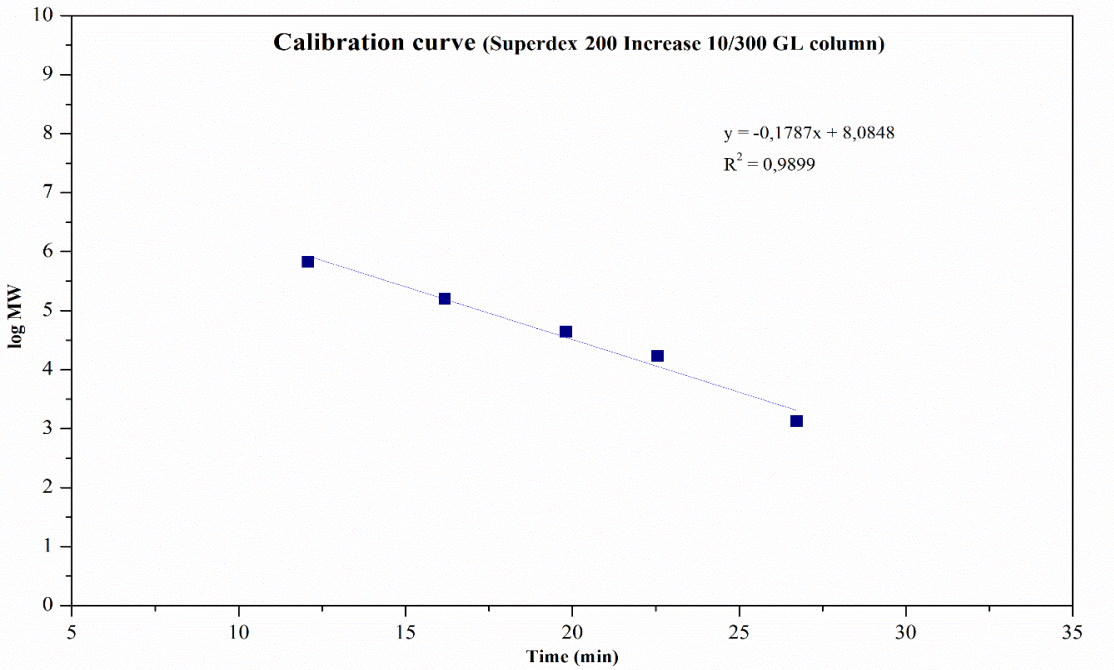

Figure 8 – Calibration curve of Gel filtration standards (Bio-Rad) used for size-exclusion chromatography on Superdex 200 Increase 10/300 GL column (GE Healthcare). Molecular weight in logarithmic scale is on y-axis, elution time of each protein standard is on x-axis.

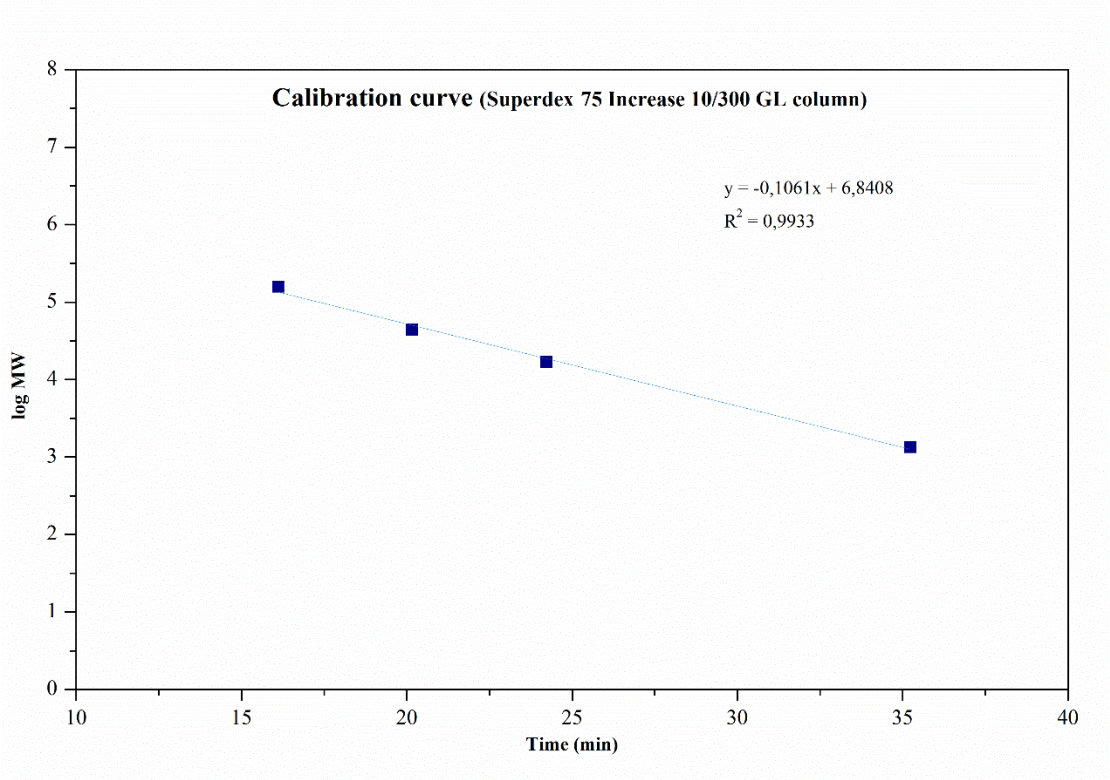

Figure 9 - Calibration curve of Gel filtration standards (Bio-Rad) used for size-exclusion chromatography on Superdex 75 Increase 10/300 GL column (GE Healthcare). Molecular weight in logarithmic scale is on y-axis, elution time of protein standard is on x-axis.

4.2.4 UV-vis spectrophotometric analysis

The second method used for protein characterization was UV-vis spectrophotometric analysis. For these experiments SPECORD S 600 diode array spectrophotometer (Analytik Jena) was used, which is designed for instant acquisitions of complete spectra in the range of 190 - 1020 nm. Recombinant proteins for these measurements were prepared by two different methods under native conditions. Non-tagged recombinant *N. gruberi* hemerythrin was isolated from inclusion bodies (see 4.2.2, page 21). Before the spectrophotometric analysis, the protein was dialyzed for 2 days in SERVAPOR® dialysis tubing against 1 000x volume of deoxygenated (purged with nitrogen) dialysis buffer (composition in Table 8, page 21) with addition of reductant sodium dithionite (Sigma) at 1mM final concentration. After dialysis, the excess sodium dithionite was removed by passage of the protein solution through Sephadex G-15 (Pharmacia) inside Poly-Prep chromatography column (Bio-Rad). Recombinant hemerythrin was then transferred to an anaerobic stoppered cuvette with micro magnetic stirring rod, purged with nitrogen and its UV-vis absorption spectra were measured on spectrophotometer. The protein was then let to autooxidise by atmospheric oxygen and UV-vis absorption spectra were continuously measured every 0,5 s till the protein was fully oxidised.

Spectrophotometric analysis of recombinant *N. gruberi* protoglobin was done with protein isolated by affinity chromatography under native conditions (see 4.1.4, page 18). Therefore, the protein contained polyhistidine tag at the C-terminus and was isolated under aerobic conditions. For measurement of UV-vis absorption spectra, protoglobin was transferred to a cuvette with stirrer. Subsequently, the cuvette with the protein was sealed and purged with nitrogen to establish anaerobic conditions. For reduction of the protein, 1mM sodium dithionite (Sigma) was added dropwise by microliter syringe (Hamilton) into the cuvette, and UV-vis absorption spectra were recorded every 0,5 s until the protoglobin was fully reduced. The protein was then let on atmospheric oxygen until the excess sodium dithionite in protein solution was fully oxidised. Afterwards, protoglobin started to autooxidise on atmospheric oxygen until its full oxidation. UV-vis absorption spectra of this whole process were continuously measured every 0,5 s. Spectrophotometric analysis of recombinant *N. gruberi* rubrerythrin was performed in the same manner as for recombinant *N. gruberi* protoglobin.

4.3 Protein localisation

4.3.1 Cell fractionation

For protein localisation analysis, cytosolic and mitochondrial fractions of *N. gruberi* were prepared by Mgr. Dominik Arbon. The well-grown culture of cells was centrifuged for 10 min, 1 200 g at room temperature. The pellet was washed with 20 ml of sucrose buffer (250mM sucrose (Lachner), 20mM MOPS (Sigma), pH 7,4). Cells were resuspended in 5 ml of sucrose buffer with added protease inhibitors cOmplete EDTA-free protease inhibitor (Roche) according to manufacturer´s protocol. The next step was sonication of cells on ice using a sonicator (QSonica Q125) at 30 % amplitude for 45 s, with 1 s pulse and 1 s pause settings. The disintegration of cells was continuously monitored with a microscope. After the majority of cells were broken, the suspension was centrifuged for 10 min, 1 200 g at 4 °C. The supernatant containing cell cytosol and intact mitochondria was centrifuged again under the same conditions as previously, followed by centrifugation for 10 min, 21 000 g at 4 °C to sediment mitochondria. The obtained supernatant was used as the cytosolic fraction. The crude mitochondrial fraction was washed twice with sucrose buffer. For both fractions the amount of proteins was determined by Bicinchoninic acid kit for protein determination (Sigma) and samples were boiled in sample buffer (composition in Table 6, page 17). Prepared fractions were analysed by SDS-PAGE and western blot using rat polyclonal antibodies against selected *N. gruberi* proteins (see chapter 4.1, page 14).

4.3.2 Slide preparation for immunofluorescence

For slide preparation, the well-grown culture of *N. gruberi* was used. The first step was the replacement of old culture medium in cultivation flask with cells with a fresh one. After this step we added mitochondrial marker MitoTracker Red CMXRos (Invitrogen) at 1:2 000 dilution and cells were incubated for 30 min in dark at 27 °C. After 30 min incubation the culture medium was again changed for a fresh one and the cells were incubated in the same manner.

Subsequently, paraformaldehyde was added to a 1 % final concentration to the cell culture and the cells were incubated for 30 min. Before further procedure cells were checked under a microscope. The fixed-cell solution was then transferred to a centrifuge tube, centrifuged for 5 min, 800 g, at room temperature and washed twice with 1 ml of PEM buffer (composition in Table 10). The cells were then blocked with 1 ml of PEMBALG buffer (composition in Table 10) for 1 h. Primary rat polyclonal antibody against *N. gruberi* rubrerythrin was added at 1:100 dilution to cells in PEMBALG buffer and cells were incubated for 1 h. After incubation the cells were washed 3x with 1 ml of PEM buffer and resuspended in 1 ml of PEMBALG buffer. A secondary donkey anti-rat IgG antibody, conjugated with Alexa fluor 488 dye, against rat immunoglobulin G (Thermo scientific) was added to cell suspension at a 1:1 000 dilution and followed by incubation for 1 h. After incubation cells were washed 3x with 1 ml of PEM buffer.

The last step was mounting the cells onto slides. Approximately 200 µl of cell suspension was gently spread onto silane-coated slides. The slides were left on air for 20 min to let cells stick onto the surface of slides. After incubation excess fluid was dried and area with cells was covered with a small drop of Vectashield solution with DAPI (Vector laboratories). Slides were covered with a degreased coverslip and analysed using a Leica TCS SP8 WLL SMD-FLIM confocal microscope. The obtained images were processed using program ImageJ 1.51.

Table 10. Composition of PEM buffer and PEMBALG buffer

PEM buffer	Concentration (mM)
PIPES (Sigma)	100,0
EGTA (Sigma)	1,0
Magnesium sulfate (Sigma)	0,1
pH 6,9	

PEMBALG buffer	Concentration
BSA (Sigma)	1 %
Lysin (Sigma)	10mM
Cold water fish skin gelatine (Sigma)	0,5 %
reagents dissolved in PEM buffer	

4.4 Functional analysis

4.4.1 Cultivation of *N. gruberi*

N. gruberi strain NEG-M was used in all experiments. Amoebas were cultivated in 25 cm^2 aerobic culture flasks with a filter (Sigma) at 27 °C. The M7 medium (composition in Table 11) used for cultivation was prepared according to (Fulton, 1974). The prepared medium was filter-sterilized, supplemented with heat-inactivated (30 min, 56 °C) fetal bovine serum (after filtration) and stored at -20 °C.

Table 11. Composition of M7 culture medium with the addition of fetal bovine serum

Reagents	Volume/mass
L-methionine (Sigma)	0,023 g
KH_2HPO_4 (Lachema)	0,181 g
$Na_2HPO_4 \cdot 12\ H_2O$ (Sigma)	0,630 g
Yeast extract (Oxoid)	2,500 g
D-glucose (Sigma)	2,700 g
Distilled water	450 ml
sterile filtered	
inactivated fetal bovine serum (Gibco)	50 ml

To determine the effect of ROS on the expression level of selected proteins, *N. gruberi* was cultivated with three different ROS-inducing compounds (phenethyl isothiocyanate (Sigma), rotenone (Sigma) and menadione (Sigma)). Approximately 200 000 cells/ml from well-grown culture were added as starting inoculum into four separate culture flasks with M7 medium. 20µM phenethyl isothiocyanate, 10µM rotenone, or 10µM menadione were added into three separate culture flasks with cells. The fourth flask was used as a negative control without the addition of any compound. Cells were cultivated under these conditions overnight at 27 °C. Concentrations of ROS-inducing compounds used in these experiments are based on previous experiments in our laboratory.

Comparative proteomic analysis of *N. gruberi* cells cultivated in different iron-containing conditions performed in our laboratory showed that the most downregulated protein in iron-limited condition is hemerythrin. To verify these results *N. gruberi* cells were cultivated in M7 medium with addition of 25µM 2,2-dipyridyl (DIP) that was used as an iron chelator to create iron-limited condition. As iron-rich control, *N. gruberi* cells were cultivated in M7 medium with 25µM ferric nitrilotriacetate (Fe-NTA). Cells were cultivated under these conditions for 72 hours at 27 °C. Concentrations of DIP and Fe-NTA used in these experiments are based on previous growth curves (Mach et al., 2018).

Similar experiment was performed with *N. gruberi* cells cultivated in different copper-containing conditions where protoglobin was identified among the most downregulated proteins in copper-limited condition while its expression increased under copper toxicity. To verify these results *N. gruberi* cells were cultivated in M7 medium with addition of 25μM bathocuproinedisulfonic acid disodium salt (BCS) that was used as specific copper chelator to create copper-limited condition. As copper-rich control, *N. gruberi* cells were cultivated in M7 medium with 25μM $CuSO_4$. Copper-toxic condition was achieved by cultivation of *N. gruberi* cells with 750μM $CuSO_4$. All cell cultures were cultivated for 72 hours at 27 °C. Concentrations of BCS and $CuSO_4$ used in these experiments are based on previous experiments in our laboratory.

Prepared cells were further processed (see chapter 4.1.6, page 20), analysed by SDS-PAGE and western blot using rat polyclonal antibodies against selected *N. gruberi* proteins (see chapter 4.1, page 14).

5 Results

5.1 Bioinformatic analysis

5.1.1 Alignment of proteins

Figure 10 shows alignment of *Naegleria gruberi* predicted protein XP_002670631.1 with hemerythrins from *Naegleria fowleri*, *Themiste hennahi*, *Sipunculus nudus*, *Phascolopsis gouldii* and *Methylococcus capsulatus*. Red rectangles point to conserved cation-coordinating residues that bind di-iron centre, based on previous study (Alvarez-Carreño et al., 2018). These residues are conserved in signal-transduction and oxygen-carrier hemerythrins.

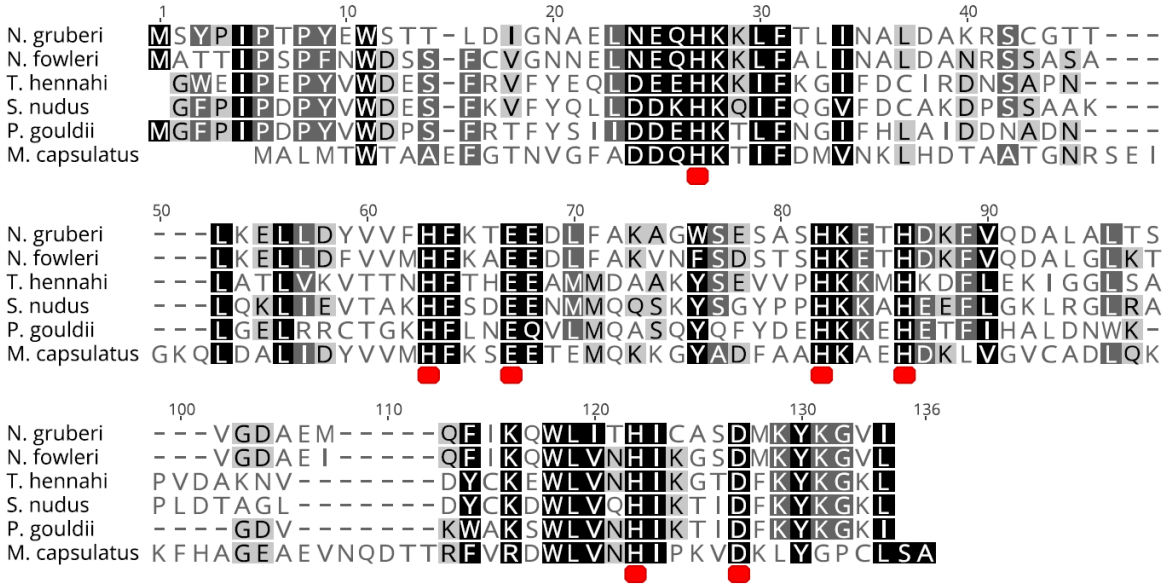

Figure 10. Alignment of *Naegleria gruberi* predicted protein (XP_002670631.1), *Naegleria fowleri* hemerythrin-like metal-binding protein (NF0127030), *Themiste hennahi* myohemerythrin (P02247), *Sipunculus nudus* myohemerythrin (Q5K473), *Phascolopsis gouldii* hemerythrin (P02244) and *Methylococcus capsulatus* bacteriohemerythrin (Q60AX2). Red rectangles mark residues that bind di-iron centre.

Figure 11 shows alignment of *Naegleria gruberi* predicted proteins XP_002677420.1 with protoglobin related proteins from *Naegleria fowleri, Methanosarcina acetivorans, Bacillus subtilis, Lobosporangium transversale, Rhizopus microsporus* and *Spizellomyces punctatus.* Red rectangles mark heme-binding proximal histidine residue which is conserved throughout all globins, and tyrosine residue, vital for oxygen-binding, based on previous study (Freitas et al., 2005).

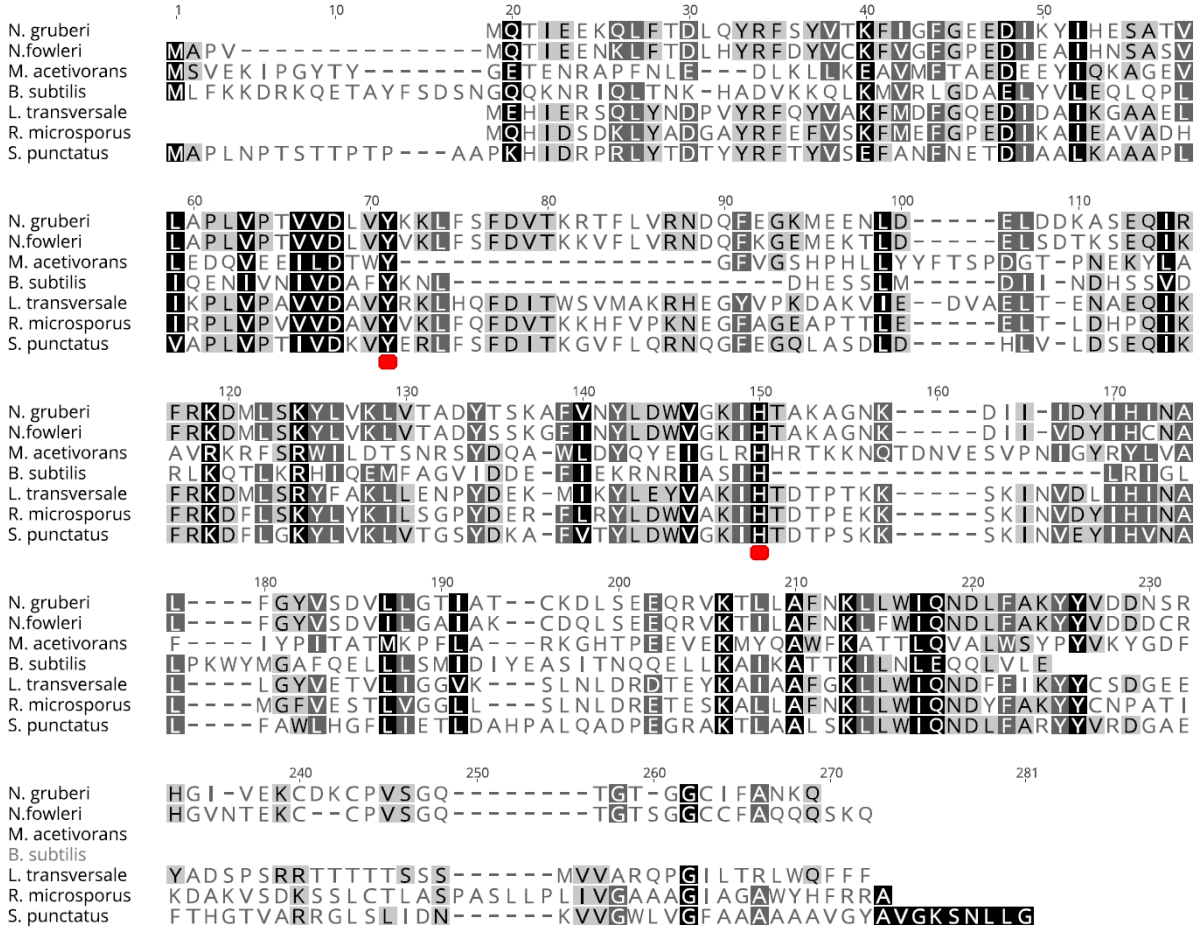

Figure 11. Alignment of *Naegleria gruberi* predicted protein (XP_002677420.1), *Naegleria fowleri* predicted protein (NF0117840), *Methanosarcina acetivorans* protoglobin (Q8TLY9), *Bacillus subtilis* heme-based aerotactic transducer HemAT (O07621), *Lobosporangium transversale* protoglobin-domain-containing protein (XP_021881135.1), *Rhizopus microsporus* hypothetical protein (XP_023470007.1) and *Spizellomyces punctatus* hypothetical protein (XP_016609942.1). Red rectangles mark tyrosine and histidine residue conserved in most globin proteins.

Figure 12 shows alignment of *Naegleria gruberi* predicted protein XP_002682904.1 with rubrerythrins from *Naegleria fowleri, Desulfovibrio vulgaris, Burkholderia pseudomallei, Entamoeba histolytica, Trichomonas vaginalis* and *Spironucleus salmonicida.* Red rectangles point to conserved cation-coordinating residues that bind di-iron centre, based on previous study (Cardenas et al., 2016). Blue rectangles mark cysteine residues of C-terminal rubredoxin domain that binds single iron which is missing in rubrerythrins from *N. gruberi*, *N. fowleri* and *B. pseudomallei.* Extensions of N-terminal parts of *N. gruberi* and *N. fowleri* proteins indicate potential mitochondrial presequence.

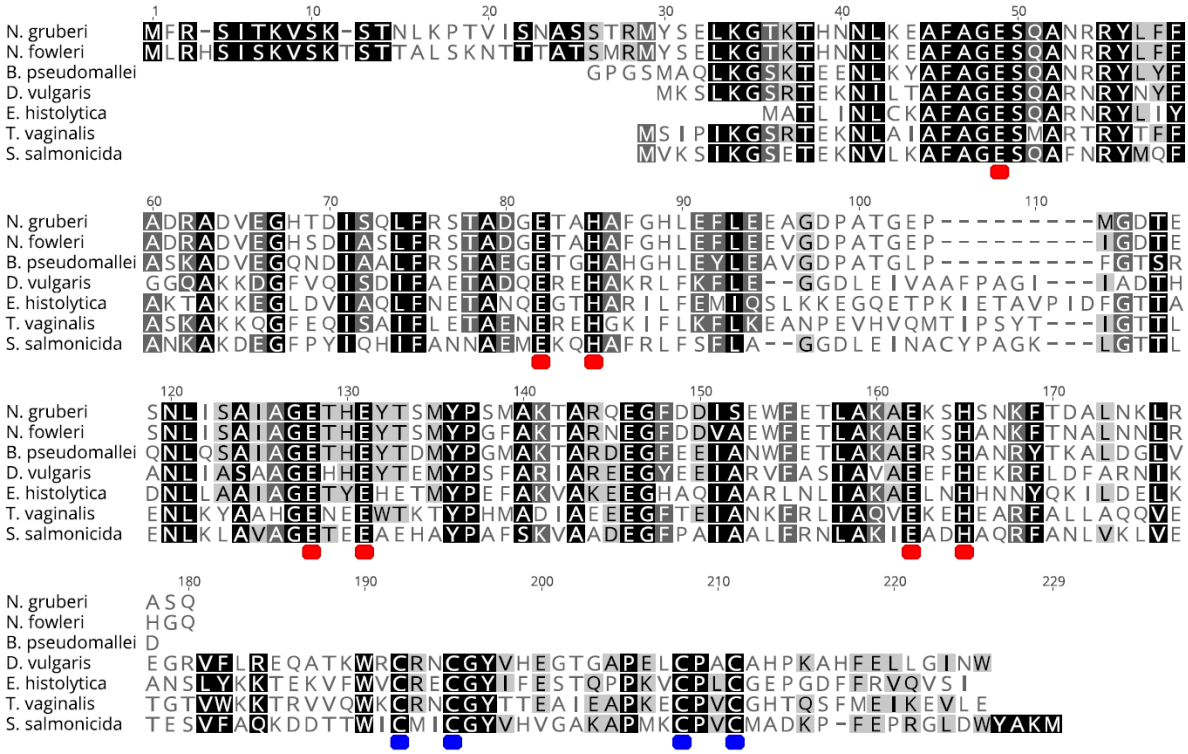

Figure 12. Alignment of *Naegleria gruberi* predicted protein (XP_002682904.1), *Naegleria fowleri* rubrerythrin (NF0040290), *Desulfovibrio vulgaris* rubrerythrin (P24931), *Burkholderia pseudomallei* rubrerythrin (4DI0), *Entamoeba histolytica* rubrerythrin (EHI_134810), *Trichomonas vaginalis* rubrerythrin (TVAG_378980) and *Spironucleus salmonicida* rubrerythrin (EST48625.1). Red rectangles mark residues that bind di-iron centre at N-terminal part of the protein. Blue rectangles mark cysteine residues of C-terminal rubredoxin domain that bind single iron.

5.1.2 Structural analysis

For better bioinformatic characterisation of examined proteins, we decided to predict their tertiary structure utilising I-TASSER server (Roy et al., 2010). This program constructs structure models and compares them with protein structures from Protein Data Bank (PDB) library. Figure 13 shows the constructed models of *Naegleria gruberi* hemerythrin (A), protoglobin (B) and rubrerythrin (C) with their structurally closest counterpart from PDB library. Predicted *N. gruberi* hemerythrin model (A) is structurally most related to myohemerythrin from *Themiste hennahi* (2MHR). Both proteins consist of four alfa-helixes with di-iron centre in the middle. Constructed *N. gruberi* protoglobin model (B) is structurally closest to *Methanosarcina acetivorans* protoglobin (2VEB). Both of these proteins contain heme as their ligand. The last model of *N. gruberi* rubrerythrin (C) is structurally closest to *Desulfovibrio vulgaris* rubrerythrin (1DVB). As previously described from alignment analysis, rubrerythrin from *N. gruberi* is missing C-terminal rubredoxin domain (red coloured β-sheets with iron ligand in purple on *Desulfovibrio vulgaris* rubrerythrin model). There is also visible extension of N-terminal part present in *N. gruberi* model which indicates potential mitochondrial presequence.

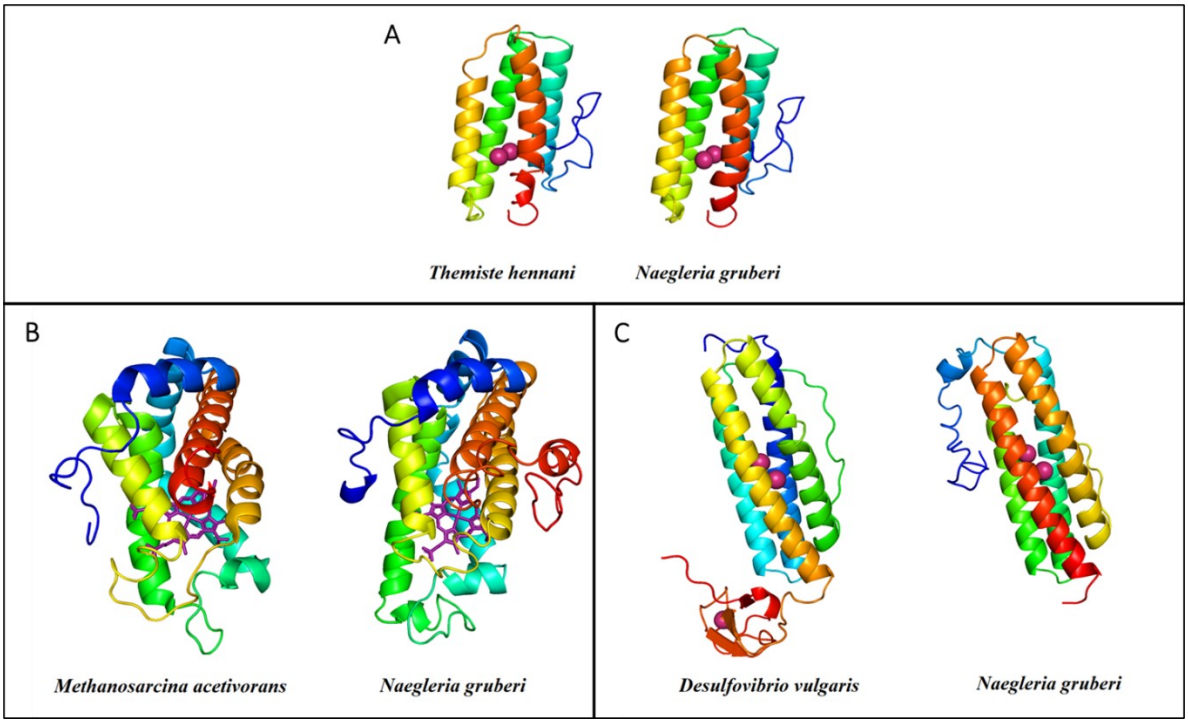

Figure 13. Predicted tertiary structures of *N. gruberi* hemerythrin (A), protoglobin (B) and rubrerythrin (C) constructed by I-TASSER server with their closest structural analogs from Protein Data Bank. N-terminal part of the proteins is coloured blue, C-terminal part is coloured red. Respective ligands for each protein, di-iron centre (A,C) and heme (B), are coloured purple.

5.2 Preparation of recombinant proteins

5.2.1 Isolation of recombinant proteins by affinity chromatography

Fractions from isolation of recombinant *N. gruberi* hemerythrin, protoglobin and rubrerythrin by affinity chromatography in native conditions were processed by SDS-PAGE. The result of this process is shown on SDS-PAGE gels stained by Coomassie Brilliant Blue G-250 in Figure 14, 15 and 16. The fraction with most protein, for each protein described in figure legend, was further processed and used as antigen to raise polyclonal antibody. For the protein characterization, protoglobin and rubrerythrin were isolated in the same manner, unlike hemerythrin, which was isolated by a different method (result at 5.3.1, page 37).

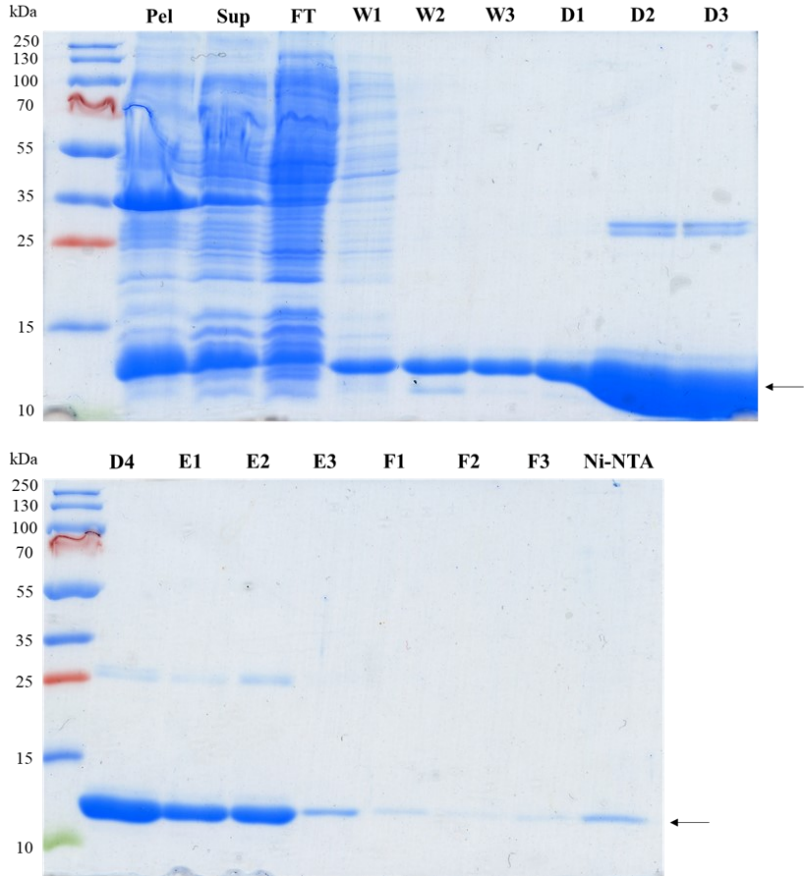

Figure 14. SDS-PAGE gel with fractions from the isolation of recombinant *N. gruberi* hemerythrin by affinity chromatography in native conditions. The size of the protein is indicated by the arrow. Fraction D3 was used for polyclonal antibody generation in experimental animal. Pel: pellet after sonication, Sup: supernatant after sonication, FT: flow-through supernatant, W1-W3: fractions after washing of matrix with wash buffer, D1-F3: fractions from elution with increasing concentration (D, E, F) of imidazole in elution buffer to release recombinant protein from the matrix, Ni-NTA: HIS-Select Nickel Affinity Gel matrix after elution.

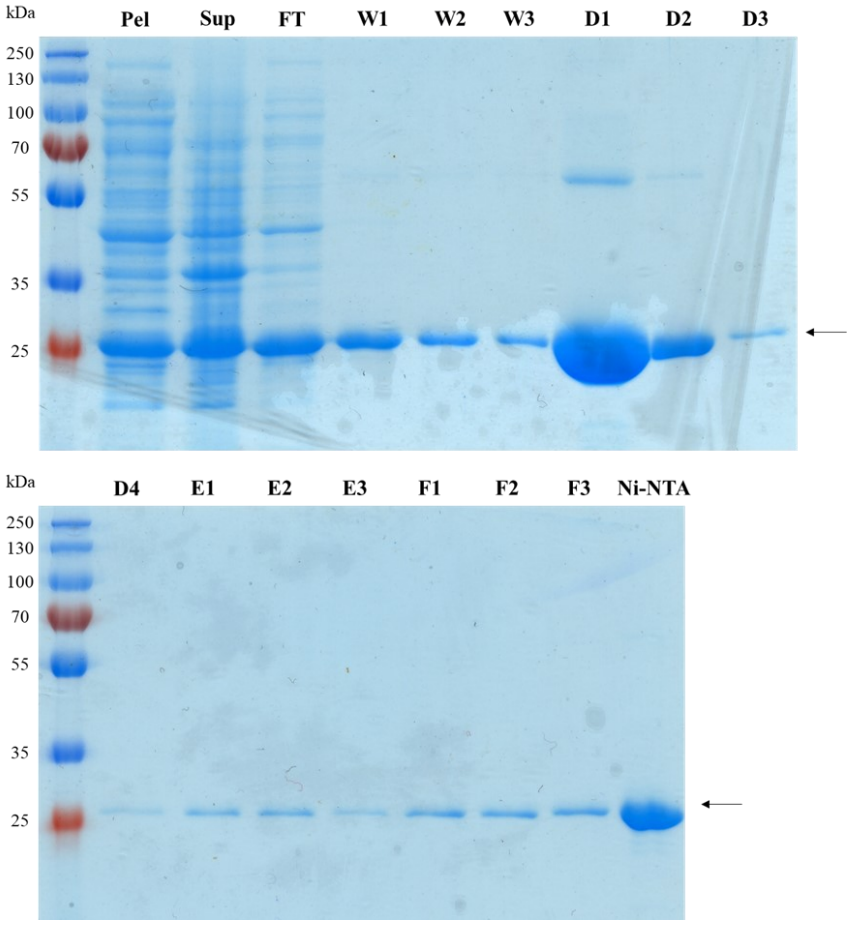

Figure 15. SDS-PAGE gel with fractions from the isolation of recombinant *N. gruberi* protoglobin by affinity chromatography in native conditions. The size of the protein is indicated by the arrow. Fraction D1 was used for polyclonal antibody generation in experimental animal. Pel: pellet after sonication, Sup: supernatant after sonication, FT: flow-through supernatant, W1-W3: fractions after washing of matrix with wash buffer, D1-F3: fractions from elution with increasing concentration (D, E, F) of imidazole in elution buffer to release recombinant protein from the matrix, Ni-NTA: HIS-Select Nickel Affinity Gel matrix after elution.

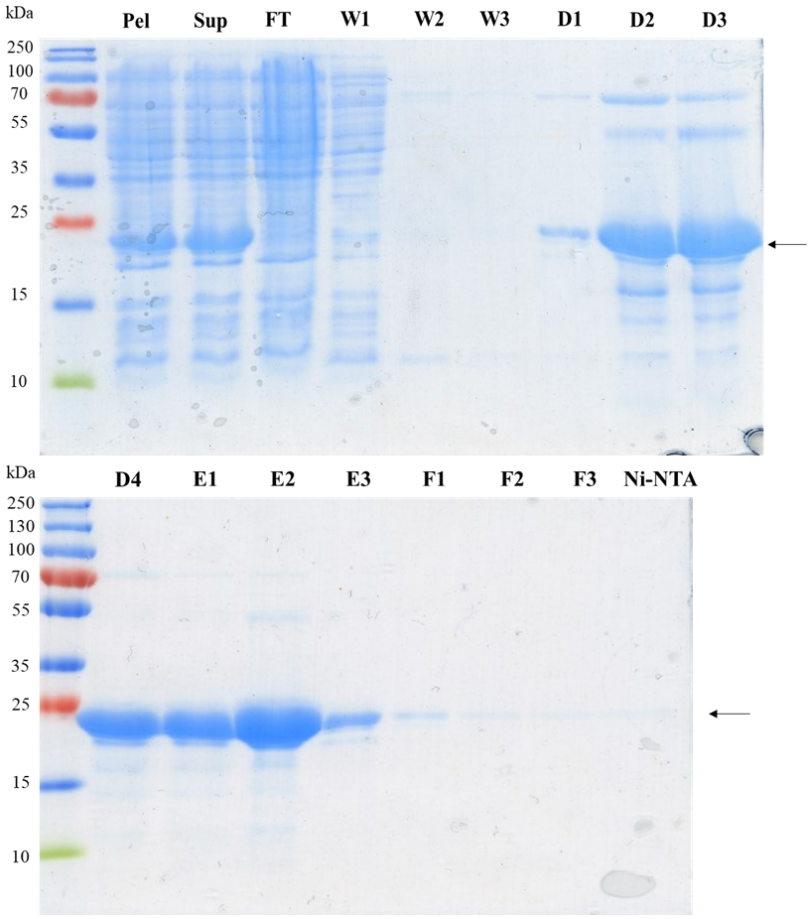

Figure 16. SDS-PAGE gel with fractions from the isolation of recombinant *N. gruberi* rubrerythrin by affinity chromatography in native conditions. The size of the protein is indicated by the arrow. Fraction E2 was used for polyclonal antibody generation in experimental animal. Pel: pellet after sonication, Sup: supernatant after sonication, FT: flow-through supernatant, W1-W3: fractions after washing of matrix with wash buffer, D1-F3: fractions from elution with increasing concentration (D, E, F) of imidazole in elution buffer to release recombinant protein from the matrix, Ni-NTA: HIS-Select Nickel Affinity Gel matrix after elution.

5.2.2 Test of antibodies

To test the specificity of the produced polyclonal rat antibodies against *N. gruberi* hemerythrin, protoglobin and rubrerythrin, immunoblot analysis of whole cell lysates of *N. gruberi* was performed. The three proteins were detected by chemiluminescence using primary antibodies against respective *N. gruberi* proteins in 1:500 dilution and secondary anti-rat immunoglobulin antibody conjugated with horseradish peroxidase. The resulting immunoblot is shown in Figure 17 with a clear signal corresponding to the correct size of all examined proteins.

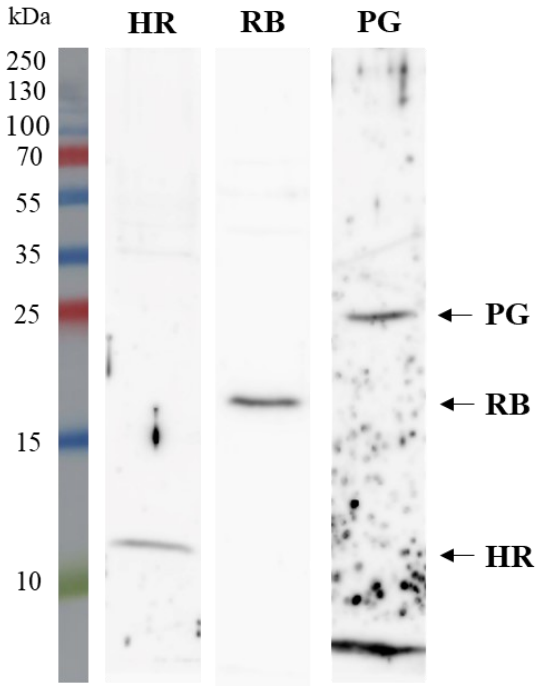

Figure 17. Immunoblot analysis of the specificity of generated antibodies against *N. gruberi* hemerythrin, protoglobin and rubrerythrin. Each line represents total cell lysate of *N. gruberi*. HR – polyclonal antibody against *N. gruberi* hemerythrin, RB – polyclonal antibody against *N. gruberi* rubrerythrin, PG – polyclonal antibody against *N. gruberi* protoglobin. The size of each examined protein is indicated by arrow.

5.3 Protein characterization

5.3.1 Isolation from inclusion bodies

Isolation of recombinant *N. gruberi* hemerythrin from inclusion bodies was used for obtaining protein without C-terminal his-tag. Reconstituted protein was later used in UV-vis spectrophotometric analysis. To check the correctness of the entire isolation process from inclusion bodies, fractions from important steps were collected, boiled in sample buffer and analysed by SDS-PAGE. The resulting Coomassie Brilliant Blue G-250 stained gel can be seen in Figure 18. The fraction 9 represents reconstituted protein isolated from inclusion bodies.

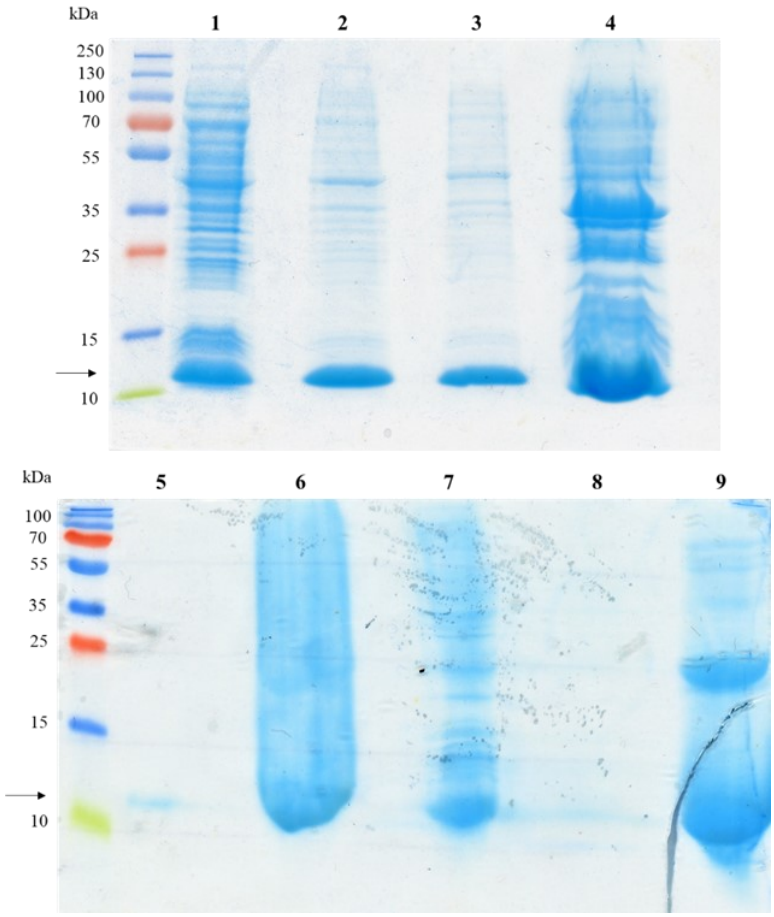

Figure 18. Fractions collected during isolation steps from inclusion bodies analysed by SDS-PAGE. 1: supernatant after sonication of bacterial pellet, 2: supernatant from the first wash of inclusion bodies with buffer containing 2M Urea, 3: supernatant from the second wash of inclusion bodies with buffer containing 2M Urea, 4: inclusion bodies after both washing steps, 5: pellet after disintegration of inclusion bodies in buffer containing 6M guanidine hydrochloride, 6: supernatant after disintegration of inclusion bodies, 7: precipitate incurred during dialysis, 8: flow-through incurred during concentration of dialysed protein with Amicon Ultra-4 centrifugal filter unit (Merck), 9: reconstituted concentrated protein.

5.3.2 Size-exclusion chromatography

Review of the literature revealed that hemerythrin can produce different types of oligomers. Marine invertebrates have two main oligomer types of hemerythrin - monomeric in their muscles and octameric in their circulatory system (Klippenstein, 1980). We thus decided to determine what type of oligomeric structures is *N. gruberi* hemerythrin forming. To achieved this, we used size-exclusion chromatography method. The ENrich SEC 70 10/300 column (Bio-Rad) was calibrated by a set of standards with known molecular weight and the isolated recombinant protein was loaded onto the column. Using the calibration curve of standards retention time and their molecular weight we calculated the molecular weight of hemerythrin in obtained elution fractions. Figure 19 shows chromatogram of recombinant *N. gruberi* hemerythrin with three distinguished peaks in UV spectrum corresponding to trimer, dimer and the most abundant monomer.

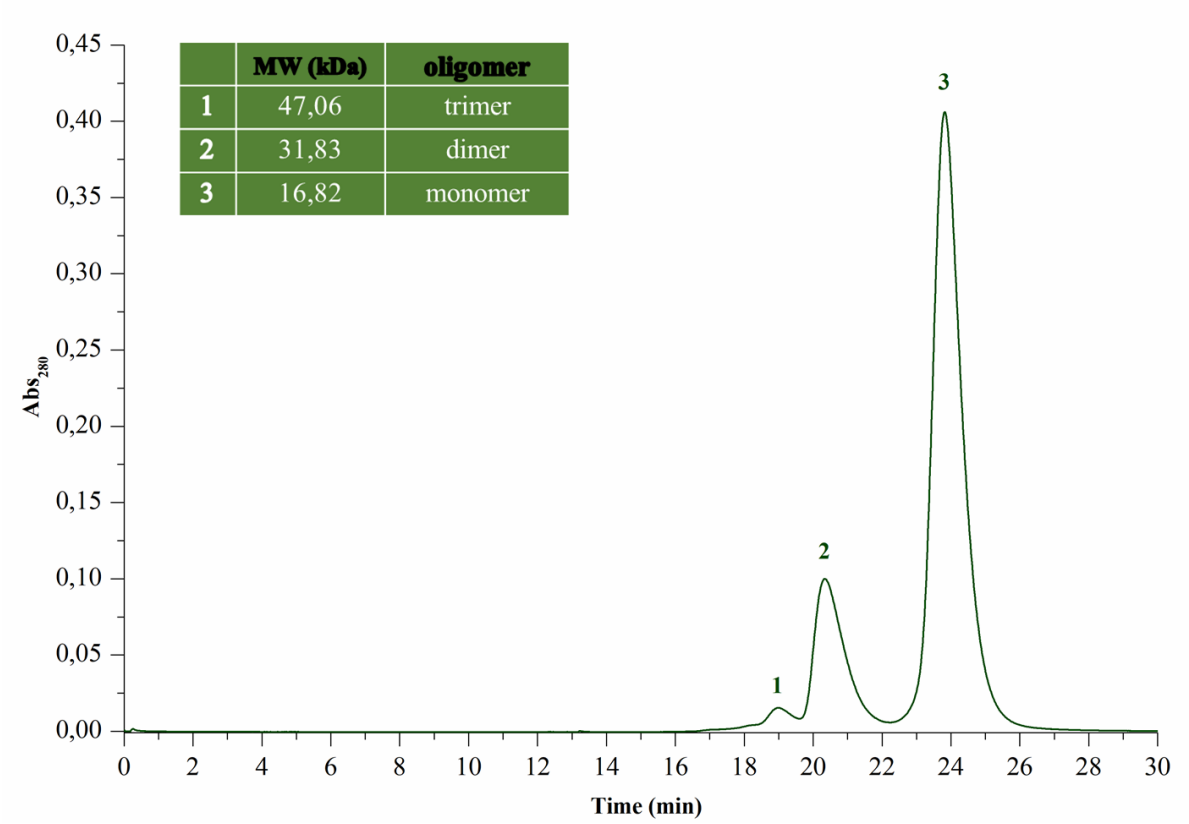

Figure 19. Chromatogram from size-exclusion chromatography of recombinant *N. gruberi* hemerythrin with a table containing the calculated molecular weight of each significant peak. The respective size corresponding to each peak was calculated from Gel filtration standards (Bio-Rad) calibration curve (see chapter 4.2.3, page 22).

Rubrerythrins from bacteria have been described to form homodimers (Wakagi, 2003). Therefore we aimed to verify that recombinant *N. gruberi* rubrerythrin is capable of producing similar oligomers. The Superdex 75 Increase 10/300 column (GE Healthcare) was used for size-exclusion chromatography. Unlike in previous analysis with hemerythrin, we observed only single peak in UV spectrum that was calculated to correspond to dimer. The chromatogram can be seen in Figure 20.

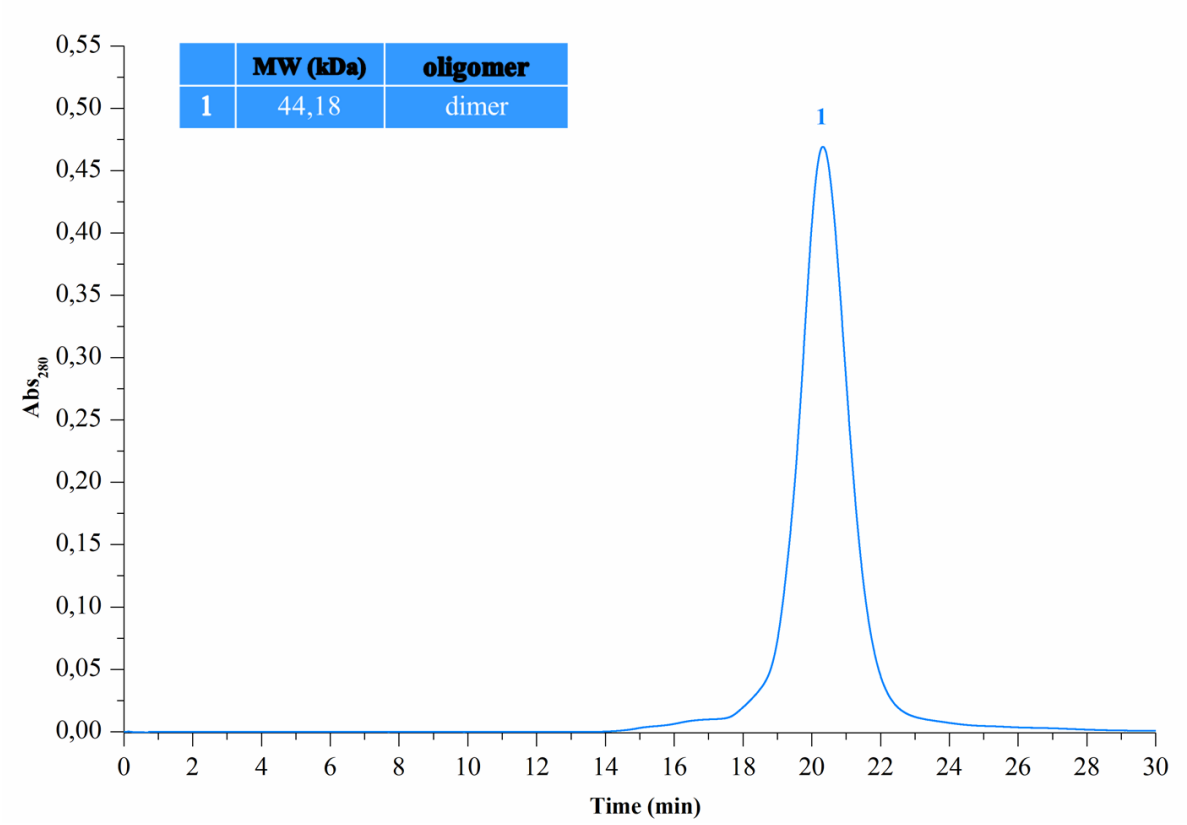

Figure 20. Chromatogram from size-exclusion chromatography of recombinant *N. gruberi* rubrerythrin with a table containing calculated molecular weight of single significant peak. The respective size corresponding to this peak was calculated from Gel filtration standards (Bio-Rad) calibration curve (see chapter 4.2.3, page 22).

The same procedure was done for recombinant *N. gruberi* protoglobin, as the most studied protoglobin from *Methanosarcina acetivorans* has been described to form homodimer (Abbruzzetti et al., 2012). Since the molecular weight of *N. gruberi* protoglobin monomer is higher than that of hemerythrin and rubrerythrin, we decided to use Superdex 200 Increase 10/300 GL column (GE Healthcare) with bigger separation range. Figure 21 shows chromatogram of recombinant *N. gruberi* protoglobin with four distinguished peaks corresponding to two big multimers, pentamer and most abundant dimer. The table within chromatogram contains the calculated molecular weight of each peak and their predicted oligomeric state.

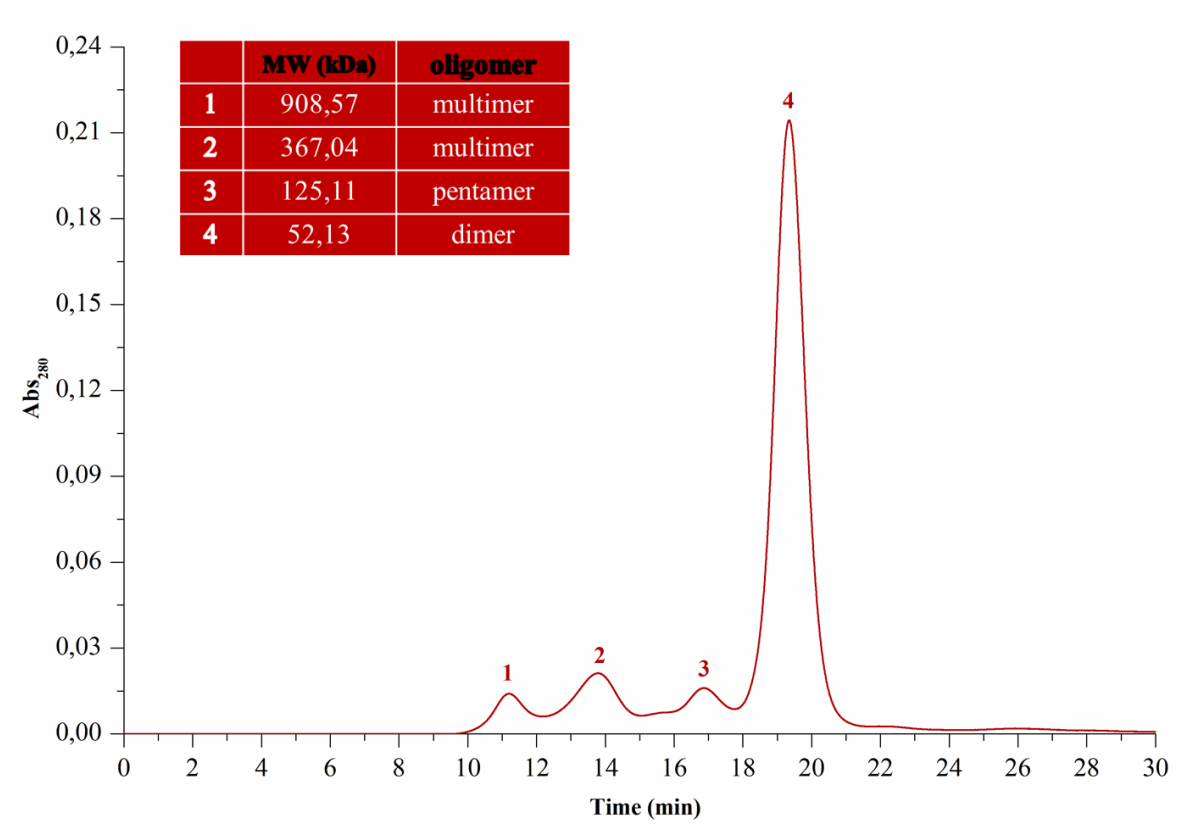

Figure 21. Chromatogram from size-exclusion chromatography of recombinant *N. gruberi* protoglobin with a table containing calculated molecular weight of each significant peak. The respective size corresponding to each peak was calculated from Gel filtration standards (Bio-Rad) calibration curve (see chapter 4.2.3, page 22).

5.3.3 UV-vis spectrophotometric analysis

Both hemerythrin and protoglobin have been described to be able to react with molecular oxygen. For verification of this reaction, we used UV-vis spectrophotometry. We prepared reduced recombinant deoxyhemerythrin from *N. gruberi* by dialysis against the excess amount of sodium dithionite (see chapter 4.2.4, page 24) and subjected it to autooxidation on air. Spectral changes during this autoxidation can be seen in Figure 22. Local absorption maxima of oxyhemerythrin at 325 nm and 375 nm indicate the presence of di-iron centre typical for hemerythrin (Kao et al., 2008). For verification of methemerythrin form we let the fully oxidised oxyhemerythrin on air for further 15 min. UV-vis spectra for the three different forms of recombinant *N. gruberi* hemerythrin can be seen in Figure 23.

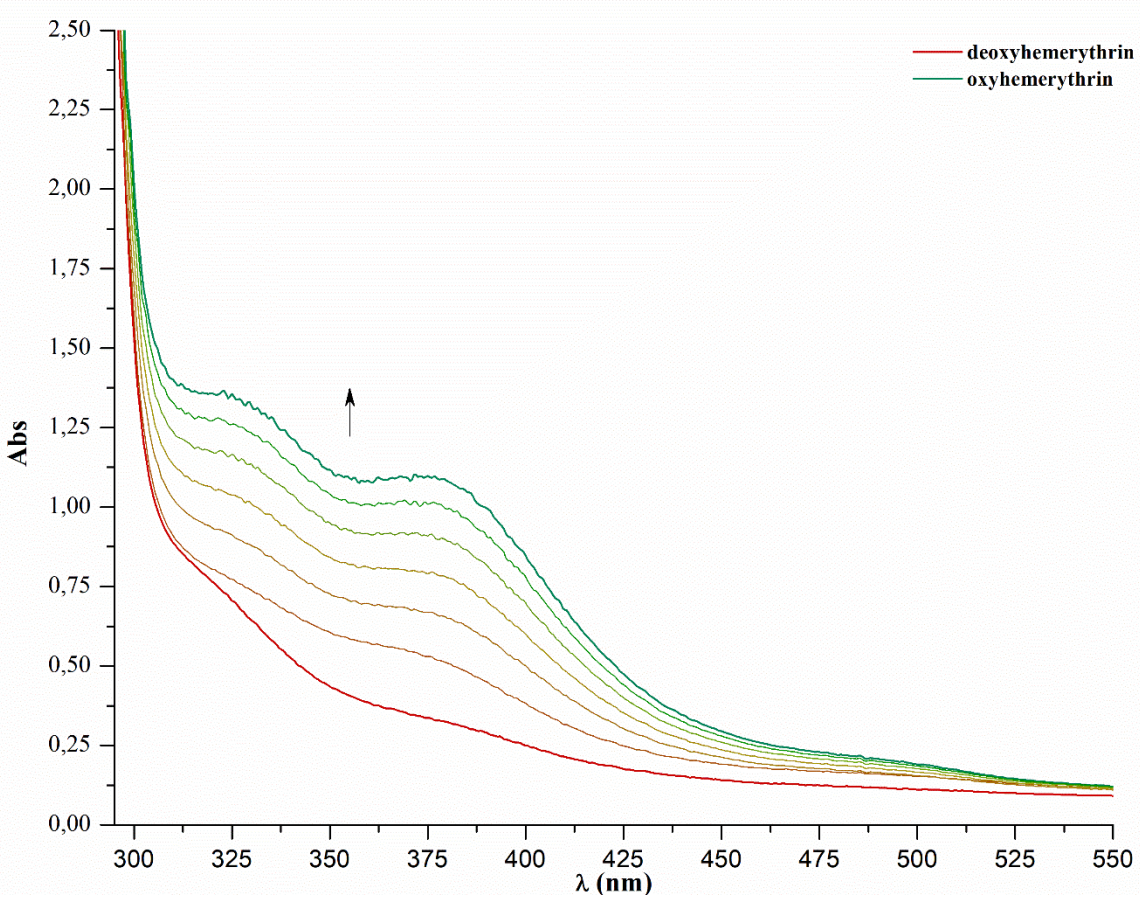

Figure 22. Spectral changes of recombinant deoxyhemerythrin (red line) from *Naegleria gruberi* in the presence of atmospheric oxygen. Oxyhemerythrin (green line) can be recognised by absorption maxima at 325 nm and 375 nm. The direction of spectral change is indicated by the arrow. The whole process took approximately 10 min.

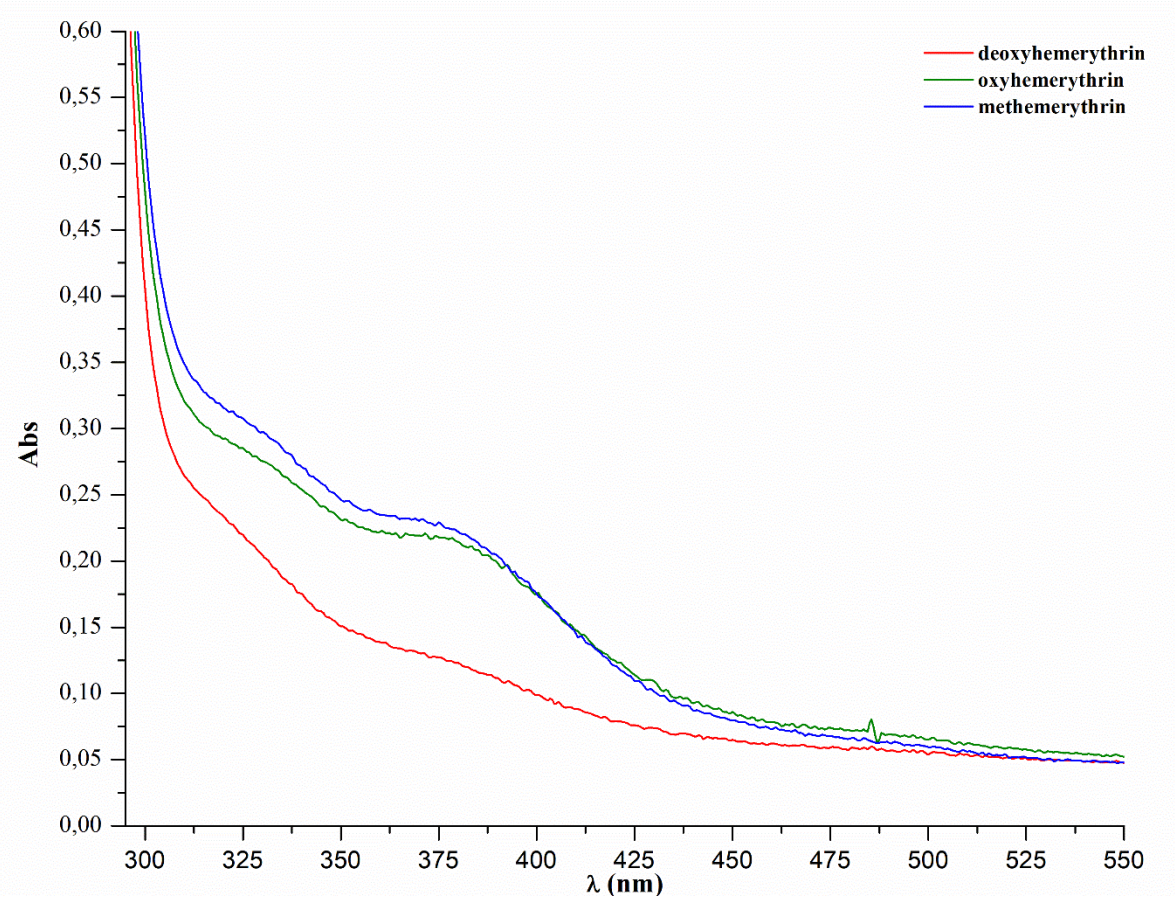

Figure 23. UV-vis spectra of recombinant *N. gruberi* hemerythrin. Difference between oxyhemerythrin (green line) and methemerythrin (blue line) is in a small shift of di-iron centre absorbance (325 nm and 375 nm) and small change of absorbance at 500 nm which indicates O_2 association. Deoxyhemerythrin (red line) was prepared by dialysis against an excess amount of sodium dithionite.

Recombinant *N. gruberi* protoglobin was isolated by affinity chromatography under aerobic conditions. Protein was reduced by the dropwise addition of sodium dithionite into the measuring cuvette till the protein was completely reduced. The whole reduction process, continuously measured by UV-vis spectrophotometer, can be seen in Figure 24. For oxidation measurement we let excess sodium dithionite in the measuring cuvette to oxidise on air. After this process, protein started to autoxidise on air which can be seen in Figure 25.

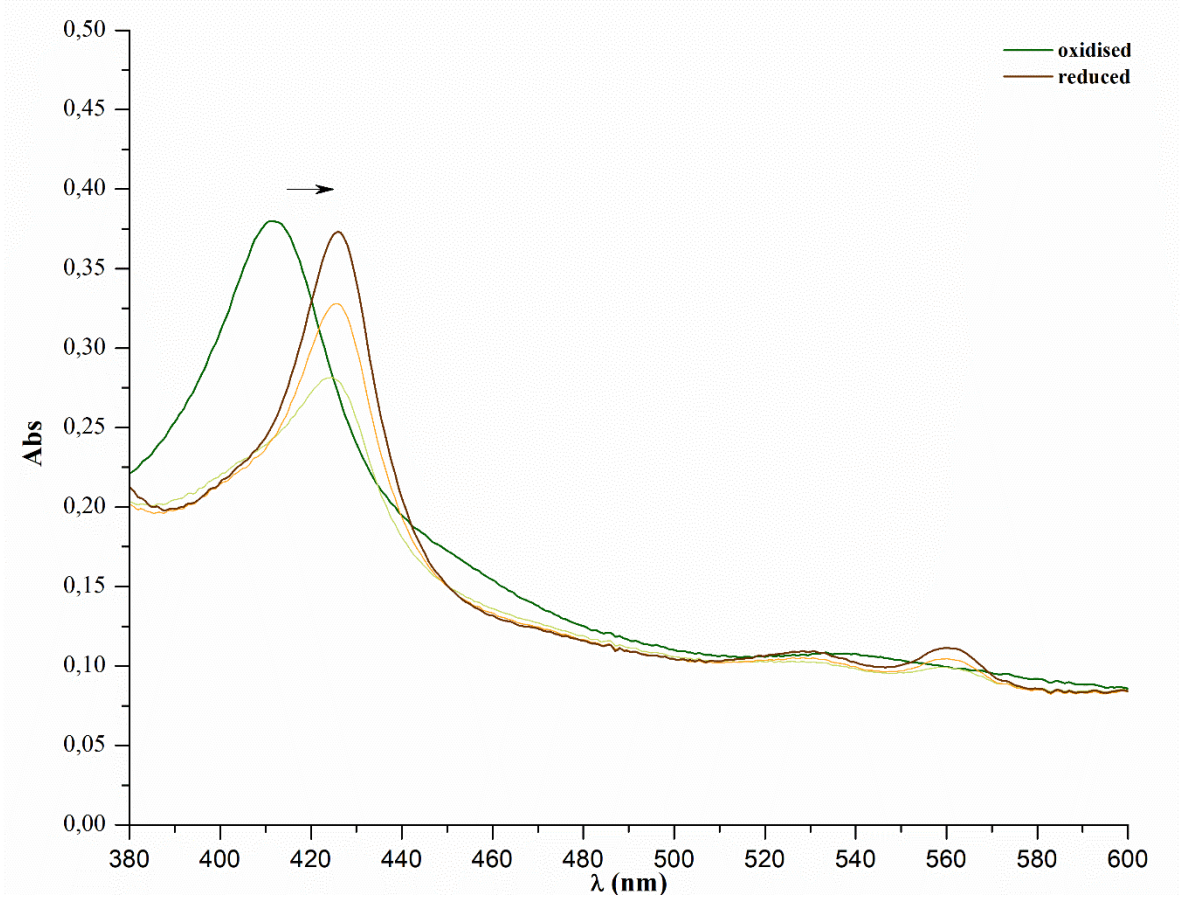

Figure 24. Spectral changes of recombinant *N. gruberi* protoglobin during reduction by dropwise addition of sodium dithionite. Oxidised state (green line) has a significant Soret absorption band at 410 nm (typical for porphyrin containing proteins (Bertini et al., 2007)). During reduction, this absorption band shifts to 430 nm and is accompanied by formation of two additional absorption bands at 530 nm and 560 nm in reduced state (brown line). The direction of spectral change is indicated by the arrow.

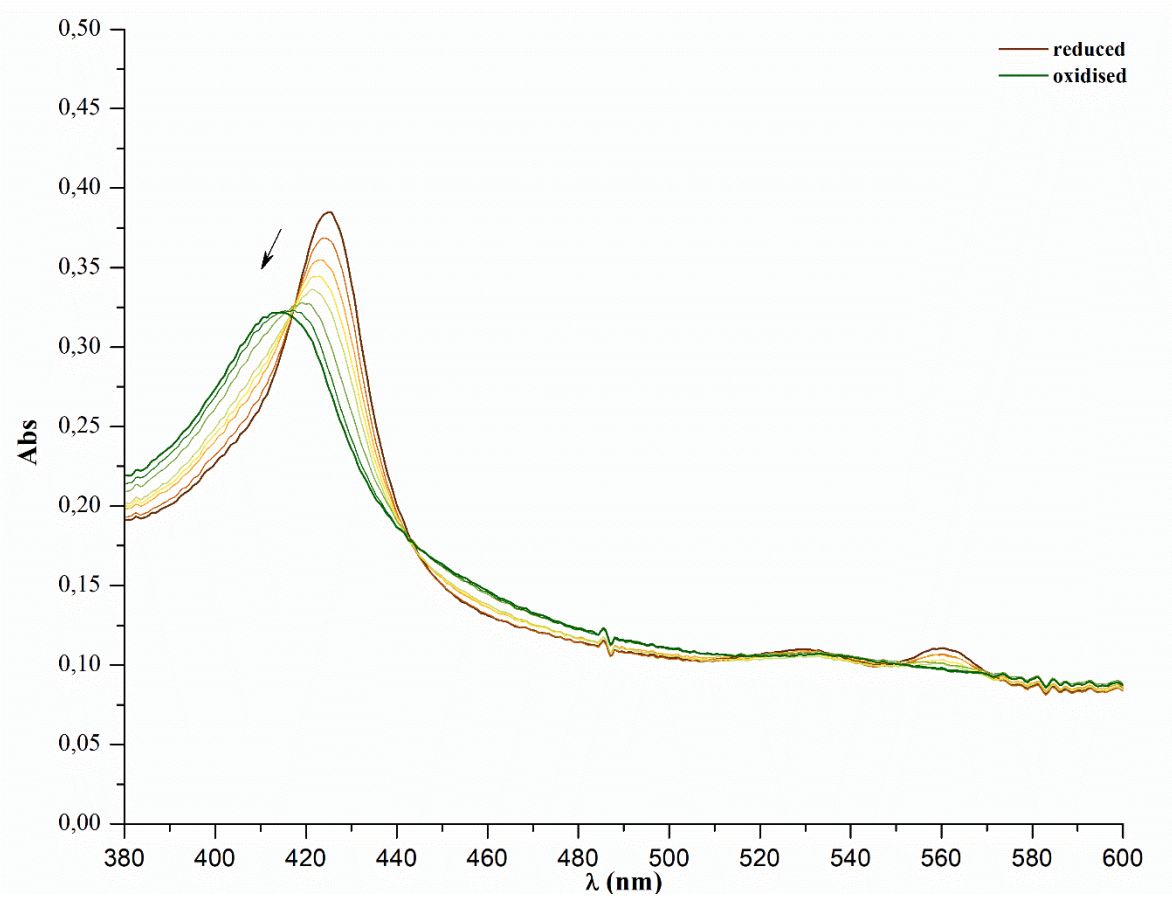

Figure 25. Autoxidation of recombinant *N. gruberi* protoglobin after removal of excess sodium dithionite. During oxidation, Soret absorption band at 430 nm in reduced state (brown line) slowly shifts back to 410 nm. as well as absorption bands at 530 nm and 560 nm start to slowly disappear. The direction of the whole process is indicated by the arrow.

The last studied protein, *N. gruberi* rubrerythrin, was also isolated by affinity chromatography under aerobic conditions. Unfortunately, reduction of this protein with sodium dithionite under anaerobic conditions wasn´t successful as the protein started to precipitate in high concentrations of sodium dithionite. UV-vis spectra of isolated recombinant rubrerythrin with local maxima at 325 nm and 375 nm corresponding to di-iron centre (Sato et al., 2012) can be seen in Figure 26.

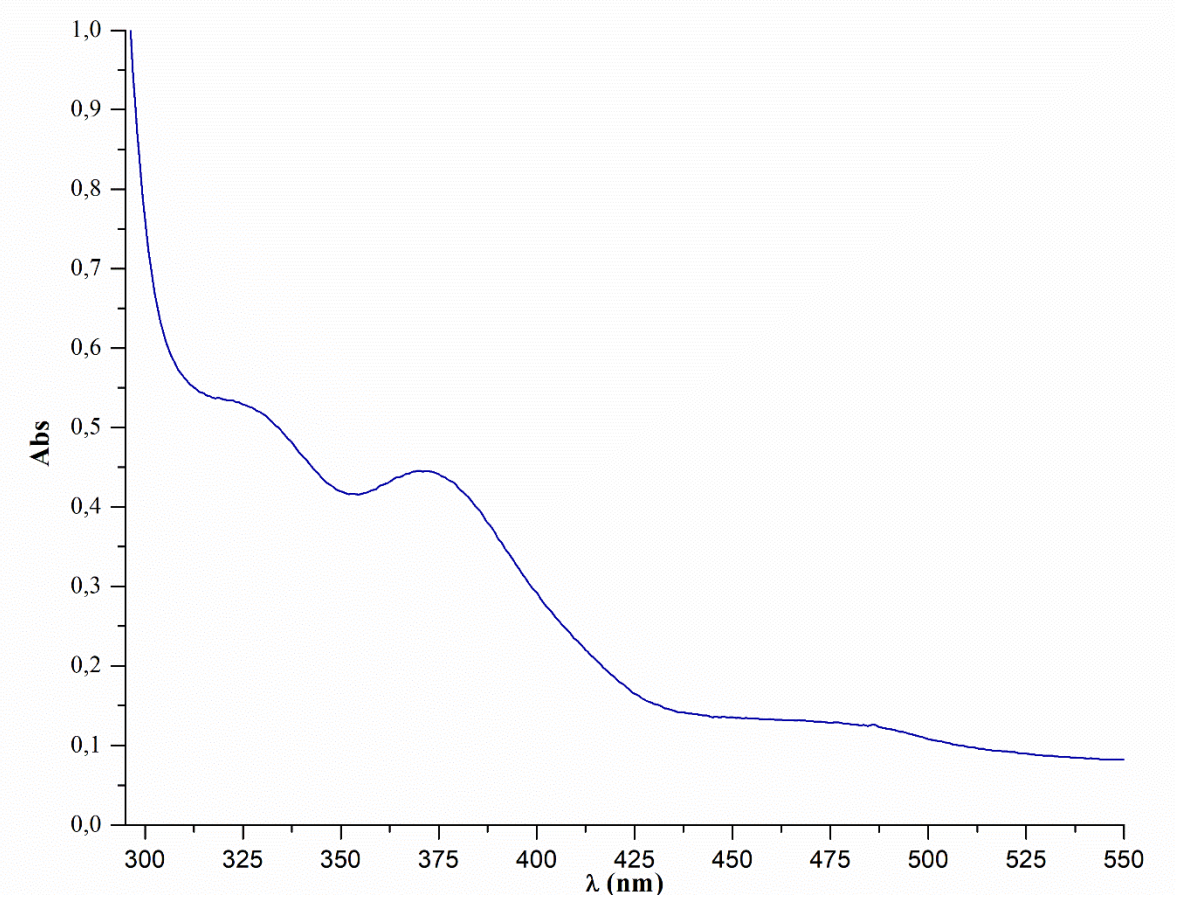

Figure 26. UV-vis absorption spectra of recombinant *N. gruberi* rubrerythrin under aerobic conditions with local maxima at 325 nm and 375 nm corresponding to di-iron centre (Sato et al., 2012).

5.4 Protein localisation

5.4.1 Cellular fractionation

We used two different approaches to determine the localisation of studied proteins. Firstly, we performed a simple cellular fractionation of *N. gruberi* cells and analysed the fractions using polyclonal antibodies against *N. gruberi* hemerythrin, protoglobin and rubrerythrin. Suitability of this method was demonstrated in one of our previous work (Mach et al., 2018) where alternative oxidase was used as a mitochondrial marker and hydrogenase maturase as a cytosolic marker. Figure 27 shows immunoblots with the three antibodies. Both hemerythrin and protoglobin have a significant band in cytosolic fraction indicated by an arrow. The result for rubrerythrin is unclear; bands are present in both cytosolic and crude mitochondrial fraction indicating e.g. leakage of mitochondrial matrix proteins. Therefore, we decided to try immunofluorescence method for determination of rubrerythrin localisation (see chapter 5.4.2, page 47).

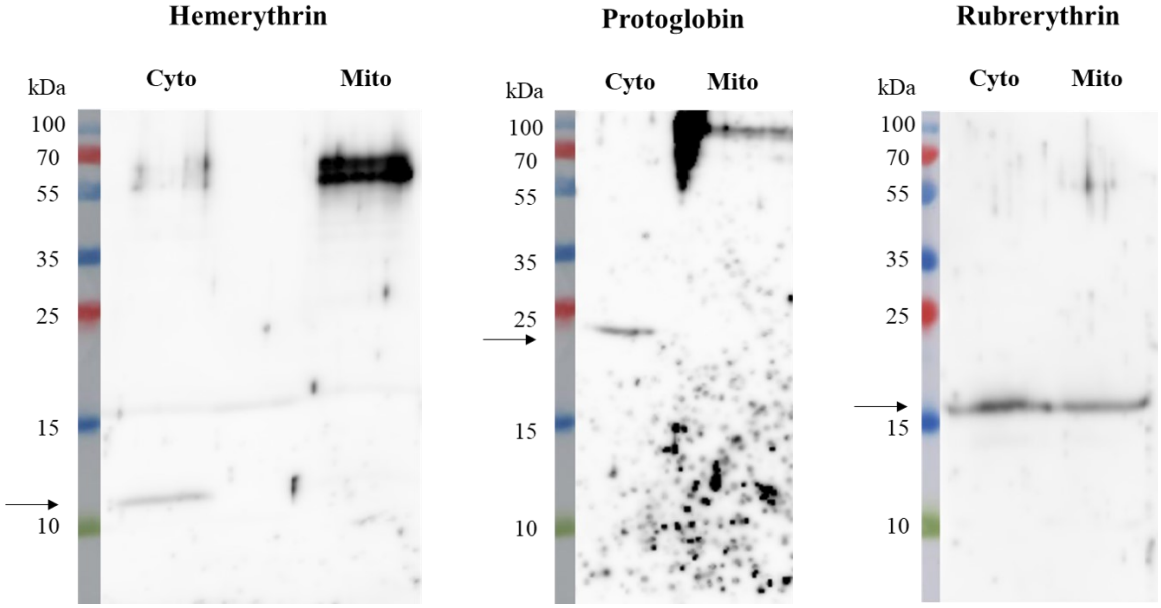

Figure 27. Immunoblot analysis of cellular localisation of three *N. gruberi* proteins (hemerythrin, protoglobin, rubrerythrin) using antibodies against these proteins. Hemerythrin and protoglobin seem to be localised in the cytosol as arrows indicate bands of the corresponding size. The localisation of rubrerythrin is inconclusive as band for this protein, indicated by the arrow, is present in both fractions. Cyto: represents a cytosolic fraction. Mito: represents a mitochondria-enriched fraction. To ensure the same amount of total loaded protein (20 µg) in each condition, protein concentration was determined by Bicinchoninic acid kit for protein determination (Sigma).

5.4.2 Immunofluorescence

The result of the immunofluorescent visualization of the *N. gruberi* rubrerythrin (NgRb) can be seen in Figure 28. Labelling of rubrerythrin was achieved using polyclonal rat antibody (see chapter 4.1, page 14). The merged image shows that rubrerythrin co-localises with MitoTracker-labelled mitochondria (Mito). Our bioinformatic prediction of *N. gruberi* rubrerythrin mitochondrial localisation seems to be correct.

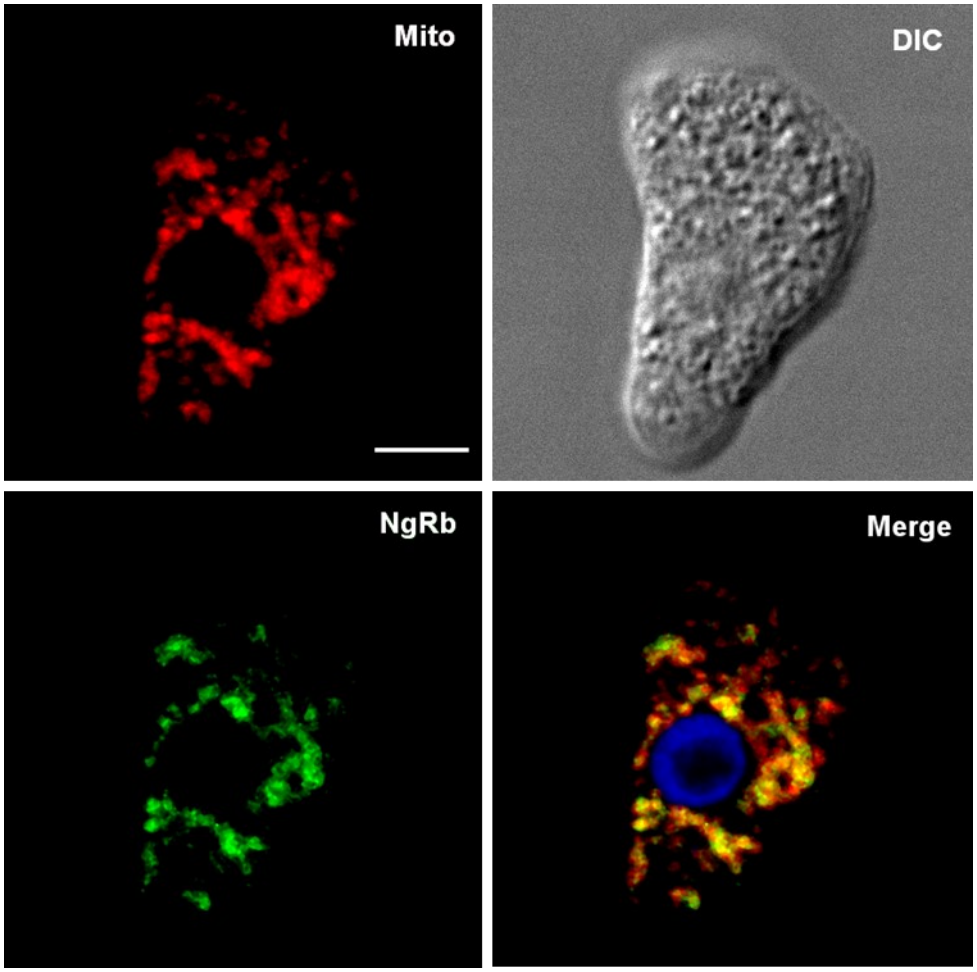

Figure 28. Cellular localisation of *N. gruberi* rubrerythrin determined by immunofluorescence. MitoTracker Red CMXRos (Invitrogen) was used for mitochondria (Mito) visualization. Rubrerythrin (NgRb) localisation was determined using polyclonal antibody against *N. gruberi* rubrerythrin (in 1:100 dilution) and a secondary antibody conjugated with Alexa fluor 488 dye. Merge represents a combination of both channels with DAPI-labelled nucleus. DIC represents differential interference contrast, scale bar is set to 5 μm.

5.5 Functional analysis

In order to test the potential role of *N. gruberi* rubrerythrin in detoxification of reactive oxygen species that was described in bacteria (Coulter et al., 1999), we cultivated *N. gruberi* cells with three different ROS-inducing compounds: rotenone, menadione and phenethyl isothiocyanate (see chapter 4.4, page 27). The resulting whole cell lysates were analysed by SDS-PAGE and western blot using rat polyclonal antibody against *N. gruberi* rubrerythrin. The aim was to determine the relationship between stress conditions and changes in the expression level of the protein. Figure 26 shows result of representative immunoblot with increase in the expression level of *N. gruberi* rubrerythrin in cells treated with ROS-inducing compounds compared to control cells, indicating the role of this protein in defence against ROS. The function of hemerythrin and protoglobin in *N. gruberi* is much less predictable as they are generally described as oxygen binding/sensing proteins. Nevertheless, from a comparative proteomic analysis of *N. gruberi* cells cultivated in different iron conditions performed in our laboratory, we discovered that the most downregulated protein in iron-limited conditions is hemerythrin. In a similar experiment with *N. gruberi* cells cultivated in different copper conditions, protoglobin was identified among the most downregulated protein in copper-limited conditions, while its expression was increased under copper toxicity. For verification of these results we decided to use western blot analysis with generated polyclonal antibodies against *N. gruberi* hemerythrin and protoglobin. Since the antibody against *N. gruberi* hemerythrin can detect this protein also in *N. fowleri* lysates, these were included in the experiment. The resulting immunoblots can be seen in Figure 30.

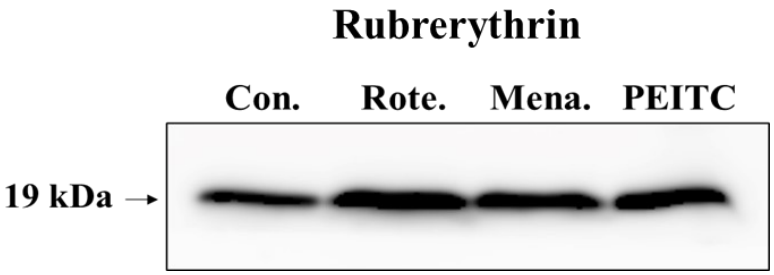

Figure 29. Result of immunoblot detection of *N. gruberi* whole cell lysates cultivated in different ROS-inducing compounds, using rat polyclonal antibody against *N. gruberi* rubrerythrin. Con.: represents *N. gruberi* cells cultivated without addition of any compound, Rote.: *N. gruberi* cells cultivated with 10µM rotenone overnight, Mena.: *N. gruberi* cells cultivated with 10µM menadione overnight, PEITC: *N. gruberi* cells cultivated with 20µM phenethyl isothiocyanate overnight. The size of *N. gruberi* rubrerythrin is indicated by arrow. To ensure the same amount of total loaded protein (20 µg) in each condition, protein concentration was determined by Bicinchoninic acid kit for protein determination (Sigma).

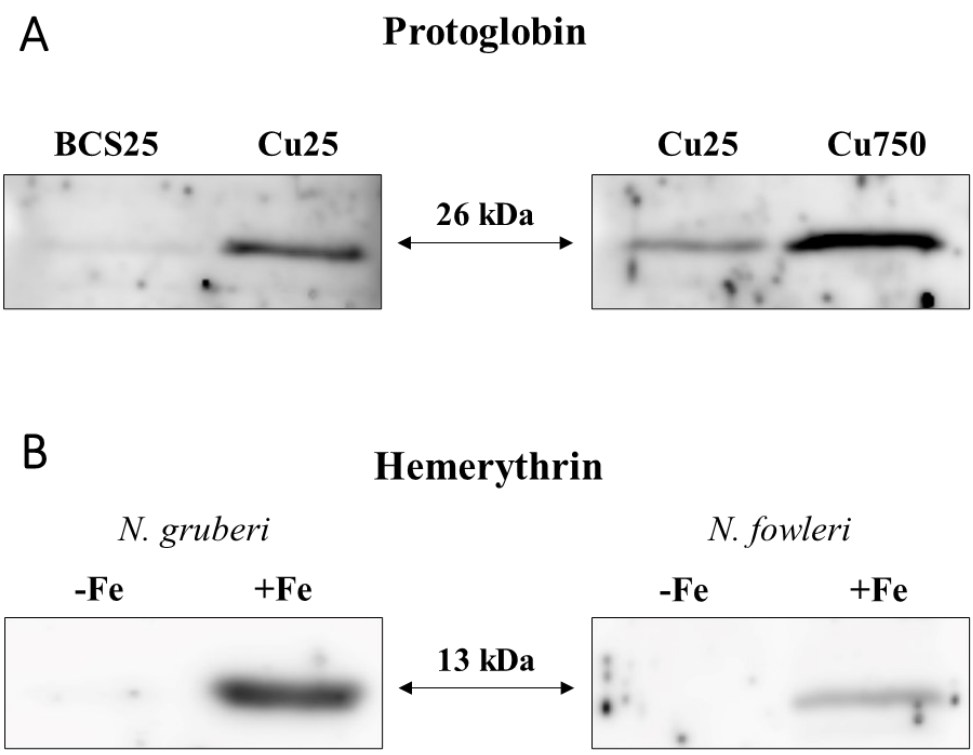

Figure 30. Result of immunoblot analysis of *Naegleria* whole cell lysates from cultures cultivated in (A) different copper-containing conditions, using rat polyclonal antibody against *N. gruberi* protoglobin and (B) different iron-containing conditions, using rat polyclonal antibody against *N. gruberi* hemerythrin. BCS25: copper-limited conditions with *N. gruberi* cells cultivated with 25µM BCS; Cu25: copper-rich conditions with *N. gruberi* cells cultivated with 25µM $CuSO_4$; Cu750: copper-toxic conditions with *N. gruberi* cells cultivated with 750µM $CuSO_4$; -Fe: iron-limited conditions with *N. gruberi* and *N. fowleri* cells cultivated with 25µM DIP; +Fe: iron-rich conditions with *N. gruberi* and *N. fowleri* cells cultivated with 25µM Fe-NTA. Cells were grown under these specific conditions for three days. To ensure the same amount of total loaded protein (20 µg) in each condition, protein concentration was determined by Bicinchoninic acid kit for protein determination (Sigma).

6 Discussion

Naegleria gruberi is an organism with interesting metabolic features. The sequenced genome revealed a number of proteins involved in the energy metabolism of anaerobic protists such as Fe-Fe hydrogenase (Fritz-Laylin et al., 2010; Opperdoes et al., 2011). These findings suggested the potential capability of *N. gruberi* to switch between aerobic and anaerobic metabolism which would help *Naegleria* to survive in an anaerobic environment. Even though the hydrogenase was shown to be active and capable of hydrogen production, its role within *N. gruberi* metabolism seems to be different than in anaerobic protists (Tsaousis et al., 2014). Apart from hydrogenase, the genome of *N. gruberi* includes a whole set of interesting proteins with unknown function and proteins whose presence in this aerobic amoeba is unexpected (Fritz-Laylin et al., 2010). In this study we focused on three such proteins: hemerythrin, protoglobin and rubrerythrin.

First of the three studied proteins, hemerythrin is annotated as predicted protein (XP_002670631.1) in the NCBI database and *N. gruberi* contains two additional paralogs of the protein (XP_002670726.1 and XP_002678794.1). Additionally, *N. fowleri* genome also contains two paralogous genes annotated as hemerythrin-like proteins (NF0119700 and NF0127030). *N. fowleri* hemerythrin (NF0127030), named Nfa1, was described as protein inducing cytotoxicity against mammalian cells in culture (Jung et al., 2009) and was localised around food vacuoles and pseudopodia of cells with a role in pathogenesis (Shin et al., 2001).

Recent studies show diverse functions of hemerythrin proteins such as iron homeostasis (Muto et al., 2017; Salahudeen et al., 2009), heavy metal detoxification (Liu et al., 2013) or oxygen sensing in bacteria (Xiong et al., 2000). The first thing we examined in this work was the capability of the protein to form oligomers. Studies made on metazoan hemerythrins revealed that a number of possible oligomeric states could be observed (Klippenstein, 1980). Utilizing size-exclusion chromatography, we showed that *N. gruberi* hemerythrin forms mainly monomeric form with a minor fraction of dimeric and trimeric forms (see chapter 5.3.2, page 38). This discovery corresponds to previous descriptions of monomeric form of myohemerythrins from muscle tissue of marine invertebrates (Klippenstein et al., 1972) and hemerythrin domain of *D. vulgaris* chemotaxis protein DcrH (Xiong et al., 2000) as well as to hemerythrin domain of human FBXL5 with both monomeric and dimeric forms (Shu et al., 2012). To demonstrate oxygen binding properties of the *N. gruberi* hemerythrin we subjected the protein to UV-vis spectroscopic analysis. We managed to verify both oxygen-binding capability and the ability of the protein to change between three characteristic redox states (see chapter 5.3.3, page 41) that have been characterised in both bacterial (Onoda et al., 2011) and metazoan hemerythrins (Garbett et al., 1969). The recombinant hemerythrin underwent rapid autooxidation when let on air which suggests its high affinity to oxygen and potential role in defence against oxidative stress. However, experiments with compounds able to induce production of reactive oxygen species did not produce a conclusive result as we were unable to see any change in protein expression (result not shown). Therefore, we still have no proof of *N. gruberi* hemerythrin

involvement in defence against oxidative stress. However, from the previous proteomic analysis of *N. gruberi* cultivated in different iron conditions, hemerythrin was identified as the most downregulated protein under iron limitation (Mach et al., 2018). The report also shows that *N. gruberi* contains only mitochondrial ferritin which seems to be the key component of mitochondrial iron homeostasis. Using generated specific antibody against hemerythrin we managed to localise the protein into the cytosol of the cells (see Figure 27, page 46) and showed that the expression of this protein is excessively downregulated in iron-limiting conditions for both *N. gruberi* and *N. fowleri* (see Figure 30, page 49) (Mach et al., 2018). Considering the fact, that *N. gruberi* cells lack cytosolic ferritin, a protein typically responsible for storage of iron, it is possible that hemerythrin undertakes ferritin's role in maintaining the homeostasis of iron outside mitochondria. This hypothesis is supported by the fact that it is a non-heme, non-iron–sulfur iron protein with a high expression level (Mach et al., 2018).

The second of the studied proteins, protoglobin, was first characterised in anaerobic methanogenic archaeon *Methanosarcina acetivorans* and aerobic hyperthermophilic archaeon *Aeropyrum pernix* as protein with capability to bind O_2, CO and NO (Allen Freitas et al., 2004). This protein belongs to globin-coupled sensor family of globins and is believed to be archetype of proteins from this family (Nardini et al., 2008). In *N. gruberi* we can find two paralogs of protoglobin (XP_002678116.1 and XP_002677420.1) both annotated as predicted proteins in the NCBI database. In comparison, *N. fowleri* genome possesses four paralogs of this protein in total (NF0061690, NF0081710, NF0108720 and NF0117840).

To characterise protoglobin (XP_002677420.1), we selected similar approach as with hemerythrin. Size exclusion chromatography analysis of recombinant *N. gruberi* protoglobin revealed dimeric form to be the most abundant, correlating with studies on *M. acetivorans* protoglobin that describe this protein to form dimers (Abbruzzetti et al., 2012; Nardini et al., 2008). Spectral analysis revealed that this protein is capable of redox reactions (see Figure 24, page 43) and the absorption spectra are suggestive of b-type heme with absorption bands at 430 nm and 460 nm (Vos et al., 2008). Autooxidation of reduced protein on air caused the shift of Soret band from 430 nm to 410 nm (see Figure 25, page 44) which has been previously described to occur with protoglobins from *M. acetivorans* and *A. pernix* (Allen Freitas et al., 2004).

From a comparative proteomic analysis of *N. gruberi* cells cultivated in different copper conditions performed in our laboratory, protoglobin was identified among the most downregulated protein under copper limiting conditions and its expression was increased when copper levels were toxic. Using specific antibody against protoglobin we show that the expression level of this protein is truly decreased in copper-limited conditions and increased in copper-toxic conditions (see Figure 30, page 49). It has been described that excess copper levels in cells can produce harmful reactive oxygen species (Pham et al., 2013). Change of protoglobin expression level in copper-toxic and copper-limited conditions and high affinity to O_2 could indicate its potential role in defence against ROS. However similarly to hemerythrin, experiments with ROS-inducing compounds did not give us

convincing result as no change in protein expression was visible (results not shown). The role in the protection against copper toxicity thus may be specific for this metal and not related directly to ROS production.

The last of the studied proteins is rubrerythrin. Rubrerythrin is a protein belonging to the ferritin-like superfamily that has been described to have peroxidase activity, implicating its role in defence against oxidative stress in anaerobic bacteria (Sztukowska et al., 2002) and anaerobic protists such as *Spironucleus salmonicida* (Stairs et al., 2019). Phylogenetic analysis of bacterial rubrerythrins revealed number of groups these proteins can be separated into, with new "aerobic-type" lineage emerging. This "aerobic-type" lineage comprises three-components: a predicted rubrerythrin-associated Fe-S oxidoreductase (RFO), a conserved protein of unknown function (DUF3501) and rubrerythrin protein lacking C-terminal rubredoxin domain arranged into a gene cluster in bacteria (Cardenas et al., 2016). Homologs of these three proteins have been also found in the newly sequenced genome of *Andalucia godoyi* with predicted mitochondrial localisation (Gray et al., 2020). In *N. gruberi* genome, we found one paralog of the rubrerythrin protein (XP_002682904.1) as well as DUF3501 (XP_002674685.1) and RFO (XP_002680212.1). All three proteins can also be found in *N. fowleri* genome (rubrerythrin (NF0040290), DUF3501 (NF0078810) and RFO (NF0017470)). In this work we mainly focused on *N. gruberi* rubrerythrin.

Number of rubrerythrins from prokaryotes has been reported to form homodimers (Jin et al., 2002; Wakagi, 2003; Weinberg et al., 2004). Utilising size exclusion chromatography analysis we verified that recombinant *N. gruberi* rubrerythrin is also able to form dimers (see Figure 20, page 39). UV-vis spectrophotometric analysis of recombinant *N. gruberi* rubrerythrin unveiled absorption spectra with local maxima at 325 nm and 375 nm corresponding to di-iron centre, analogous to hemerythrin (Kao et al., 2008). Reduction of the protein was unsuccessful as the protein precipitated in high concentrations of sodium dithionite.

Previous characterisations of rubrerythrin in *Trichomonas vaginalis*, *Entamoeba histolytica* and *Spironucleus salmonicida* localised this protein into their mitochondria-related organelles (Maralikova et al., 2010; Pütz et al., 2005; Stairs et al., 2019). Analysis of alignment of *N. gruberi* rubrerythrin with rubrerythrins from other organisms indicates the presence of potential mitochondrial targeting sequence also in *N. gruberi*. Using specific polyclonal antibody against *N. gruberi* rubrerythrin we managed to localise this protein in mitochondria (see Figure 28, page 47) which corresponds to our bioinformatic analysis and recent discovery of rubrerythrin in predicted mitochondrial proteome of *Andalucia godoyi* (Gray et al., 2020).

Rubrerythrin has been described to be a peroxidase with potential participation in defence against reactive oxygen species in bacteria (Coulter et al., 1999). We tried to evaluate whether *N. gruberi* rubrerythrin has comparable function, cultivating *N. gruberi* cells with ROS inducing compounds. Immunoblot analysis showed increased expression level of rubrerythrin under oxidative stress strongly suggesting its role in defence against ROS in *N. gruberi*.

7 Conclusion

In this work we focused on characterisation of three proteins from *N. gruberi* - hemerythrin (XP_002670631.1), protoglobin (XP_002677420.1) and rubrerythrin (XP_002682904.1). We successfully managed to clone respective genes from *N. gruberi* into expression plasmids that were then transformed into *E. coli*, subsequently expressed in the large volume and isolated by affinity chromatography in native conditions. Recombinant proteins produced by this method were used for preparation of polyclonal antibodies in experimental animals and in biochemical analysis including size-exclusion chromatography and UV-vis spectrophotometry. Results from size-exclusion chromatography provided findings comparable to previous studies on hemerythrins, protoglobins and rubrerythrins in other organisms. UV-vis spectrophotometry verified hemerythrin's and protoglobin's high affinity to oxygen. In the case of rubrerythrin further work has to be done on this matter as the protein precipitates during reduction in our conditions and we were unable to measure its whole redox reaction.

Prepared polyclonal antibodies were used to determine protein localisation in *N. gruberi* with hemerythrin and protoglobin being localised into cell cytosol. Bioinformatic analysis indicated mitochondrial localisation of rubrerythrin which was confirmed by immunofluorescence microscopy on *N. gruberi* utilising rubrerythrin polyclonal antibody. Moreover, we managed to verify previous proteomic analysis that showed strong decrease in hemerythrin expression in iron-limited conditions and changes of protoglobin expression level in copper-toxic conditions indicating their possible role in defence against reactive oxygen species or in maintaining homeostasis of these essential trace elements. Since western blot with whole cell lysates of *N. gruberi* cultivated with ROS-inducing compounds were inconclusive, we propose that the role of these proteins is more likely related to the metals themselves rather than defence against ROS production. For rubrerythrin we managed to show the changes of its expression level during stress induced by three ROS-inducing compounds. Therefore, it can be hypothesised that rubrerythrin plays role in defence against oxidative stress in *N. gruberi*.

In the future, we would like to focus on biochemical characterisation of the whole "aerobic-type" rubrerythrin three component system. Furthermore, we would like to analyse how changes in oxygen levels in the cultivation medium affect the expression of hemerythrin, protoglobin and rubrerythrin in *N. gruberi*.

8 Abbreviations

AOX	Alternative oxidase
ATP	Adenosine-5-triphosphate
BCS	Bathocuproinedisulfonic acid disodium salt
cAMP	Cyclic adenosine monophosphate
cDNA	Complementary deoxyribonucleic acid
CoA	Coenzyme A
DAPI	4,6-diamidino-2-phenylindole
DIP	2,2-Dipyridyl
DNA	Deoxyribonucleic acid
DPS	DNA protection during starvation protein
EDTA	Ethylenediaminetetraacetic acid
FBXL5	F-box and Leucine-Rich Repeat Protein 5
Fe-NTA	Ferric nitrilotriacetate
FPLC	Fast protein liquid chromatography
GSH	Glutathione
GSSG	Glutathione disulfide
HEPES	4-(2-hydroxyethyl)piperazine-1-ethanesulfonic acid
IPTG	Isopropyl β-D-1-thiogalactopyranoside
IRP2	Iron regulatory protein 2
MOPS	3-morpholinopropane-1-sulfonic acid
NADH	Reduced nicotinamide adenine dinucleotide
NADPH	Reduced nicotinamide adenine dinucleotide phosphate
NDH2	type II NADH:quinone oxidoreductase (alternative NADH dehydrogenase)
PAM	Primary amoebic meningoencephalitis
ROS	Reactive oxygen species
SDS-PAGE	Sodium dodecyl sulfate–polyacrylamide gel electrophoresis
SOD	Superoxide dismutase
TWEEN	Polyoxyethylene sorbitan monolaurate

9 References

Abbruzzetti, S., Tilleman, L., Bruno, S., Viappiani, C., Desmet, F., van Doorslaer, S., Coletta, M., Ciaccio, C., Ascenzi, P., Nardini, M., Bolognesi, M., Moens, L., & Dewilde, S. (2012). Ligation tunes protein reactivity in an ancient haemoglobin: Kinetic evidence for an allosteric mechanism in *Methanosarcina acetivorans* protoglobin. *PLoS One*, *7*(3).

Abreu, I. A., & Cabelli, D. E. (2010). Superoxide dismutases - a review of the metal-associated mechanistic variations. *Biochimica et Biophysica Acta - Proteins and Proteomics*, *1804*(2), 263–274.

Allen Freitas, T. K., Hou, S., Dioum, E. M., Saito, J. A., Newhouse, J., Gonzalez, G., Gilles-Gonzalez, M.-A., & Alam, M. (2004). Ancestral hemoglobins in Archaea. *Proceedings of the National Academy of Sciences of the United States of America*, *101*(17), 6675–6680.

Alvarez-Carreño, C., Alva, V., Becerra, A., & Lazcano, A. (2018). Structure, function and evolution of the hemerythrin-like domain superfamily. *Protein Science*, *27*(4), 848–860.

Andrews, S. C. (2010). The Ferritin-like superfamily: Evolution of the biological iron storeman from a rubrerythrin-like ancestor. *Biochimica et Biophysica Acta - General Subjects*, *1800*(8), 691–705.

Apel, K., & Hirt, H. (2004). Reactive oxygen species: Metabolism, oxidative stress and signal transduction. *Annual Review of Plant Biology*, *55*(1), 373–399.

Auten, R. L., & Davis, J. M. (2009). Oxygen toxicity and reactive oxygen species: The devil is in the details. *Pediatric Research*, *66*, 121–127.

Becuwe, P., Gratepanche, S., Fourmaux, M.-N., van Beeumenb, J., Samyn, B., Mercereau-Puijalon, O., Touzeld, J. P., Slomianny, C., Camusa, D., & Divea, D. (1996). Characterization of iron-dependent endogenous superoxide dismutase of *Plasmodium falciparum*. *Molecular and Biochemical Parasitology*, *76*, 125–134.

Bertini, I., Gray, H. B., Steifel, E. I., & Valentine, J. S. (2007). Biological inorganic chemistry: structure and reactivity. *University Science Books*

Bexkens, M. L., Zimorski, V., Sarink, M. J., Wienk, H., Brouwers, J. F., de Jonckheere, J. F., Martin, W. F., Opperdoes, F. R., van Hellemond, J. J., & Tielens, A. G. M. (2018). Lipids are the preferred substrate of the protist *Naegleria gruberi*, relative of a human brain pathogen. *Cell Reports*, *25*(3), 537-543.

Burns, J. L., Rivera, S., Deer, D. D., Joynt, S. C., Dvorak, D., & Weinert, E. E. (2016). Oxygen and bis(3',5')-cyclic dimeric guanosine monophosphate binding control oligomerization state equilibria of diguanylate cyclase-containing globin coupled sensors. *Biochemistry*, *55*(48), 6642–6651.

Cabeza, M. S., Guerrero, S. A., Iglesias, A. A., & Arias, D. G. (2015). New enzymatic pathways for the reduction of reactive oxygen species in *Entamoeba histolytica*. *Biochimica et Biophysica Acta - General Subjects*, *1850*(6), 1233–1244.

Cardenas, J. P., Quatrini, R., & Holmes, D. S. (2016). Aerobic lineage of the oxidative stress response protein rubrerythrin emerged in an ancient microaerobic, (hyper)thermophilic environment. *Frontiers in Microbiology*, *7*.

Carter, R. F. (1970). Description of a *Naegleria* sp. isolated from two cases of primary amoebic meningo-encephalitis and of the experimental pathological changes induced by it. *The Journal of Pathology*, *100*(4), 217–244.

Chaudhuri, M., Ajayi, W., & Hill, G. C. (1998). Biochemical and molecular properties of the *Trypanosoma brucei* alternative oxidase. *Molecular and Biochemical Parasitology*, *95*, 53–68.

Chen, K. H. C., Wu, H. H., Ke, S. F., Rao, Y. T., Tu, C. M., Chen, Y. P., Kuei, K. H., Chen, Y. S., Wang, V. C. C., Kao, W. C., & Chan, S. I. (2012). Bacteriohemerythrin bolsters the activity of the particulate methane monooxygenase (pMMO) in *Methylococcus capsulatus* (Bath). *Journal of Inorganic Biochemistry*, *111*, 10–17.

Chiranand, W., McLeod, I., Zhou, H., Lynn, J. J., Vega, L. A., Myers, H., Yates, J. R., Lorenz, M. C., & Gustin, M. C. (2008). CTA4 transcription factor mediates induction of nitrosative stress response in *Candida albicans*. *Eukaryotic Cell*, *7*(2), 268–278.

Coulter, E. D., Shenvi, N. v., & Kurtz, D. M. (1999). NADH peroxidase activity of rubrerythrin. *Biochemical and Biophysical Research Communications*, *255*(2), 317–323.

Das, K., & Roychoudhury, A. (2014). Reactive oxygen species (ROS) and response of antioxidants as ROS-scavengers during environmental stress in plants. *Frontiers in Environmental Science*, *2*.

de Jesús-Berríos, M., Liu, L., Nussbaum, J. C., Cox, G. M., Stamler, J. S., & Heitman, J. (2003). Enzymes that counteract nitrosative stress promote fungal virulence. *Current Biology*, *13*(22), 1963–1968.

de Jonckheere, J. F. (2006). Isolation and molecular identification of free-living amoebae of the genus *Naegleria* from Arctic and sub-Antarctic regions. *European Journal of Protistology*, *42*(2), 115–123.

de Jonckheere, J. F. (2014). What do we know by now about the genus Naegleria? *Experimental Parasitology*. *145,* 2–9

de Jonckheere, J. F., Pernin, P., Scaglia, M., & Michel, R. (1984). A comparative study of 14 strains of *Naegleria australiensis* demonstrates the existence of a highly virulent subspecies: *N. australiensis italica* n. spp. *The Journal of Protozoology*, *31*(2), 324–331.

deMaré, F., Kurtz, D. M., & Nordlund, P. (1996). The structure of *Desulfovibrio vulgaris* rubrerythrin reveals a unique combination of rubredoxin-like FeS4 and ferritin-like diiron domains. *Nature Structural Biology*, *3*, 539–546.

Dillard, B. D., Demick, J. M., Adams, M. W. W., & Lanzilotta, W. N. (2011). A cryo-crystallographic time course for peroxide reduction by rubrerythrin from *Pyrococcus furiosus*. *Journal of Biological Inorganic Chemistry*, *16*(6), 949–959.

Freitas, T. A. K., Saito, J. A., Hou, S., & Alam, M. (2005). Globin-coupled sensors, protoglobins, and the last universal common ancestor. *Journal of Inorganic Biochemistry*, *99*(1), 23–33.

Fritz-Laylin, L. K., Ginger, M. L., Walsh, C., Dawson, S. C., & Fulton, C. (2011). The *Naegleria* genome: A free-living microbial eukaryote lends unique insights into core eukaryotic cell biology. *Research in Microbiology*, *162*(6), 607–618.

Fritz-Laylin, L. K., Prochnik, S. E., Ginger, M. L., Dacks, J. B., Carpenter, M. L., Field, M. C., Kuo, A., Paredez, A., Chapman, J., Pham, J., Shu, S., Neupane, R., Cipriano, M., Mancuso, J., Tu, H., Salamov, A., Lindquist, E., Shapiro, H., Lucas, S., Grigoriev, I. V., Cande, W. Z., Fulton, Ch., Rokhsar, D. S., Dawson, S. C. (2010). The genome of *Naegleria gruberi* illuminates early eukaryotic versatility. *Cell*, *140*(5), 631–642.

Fulton, C. (1970). Amebo-flagellates as research partners: The laboratory biology of *Naegleria* and *Tetramitus*. *Methods in Cell Biology*, *4*, 341–346.

Fulton, C. (1974). Axenic cultivation of *Naegleria gruberi*: Requirement for methionine. *Experimental Cell Research*, *88*, 365–370.

Fulton, C., & Dingle, A. D. (1967). Appearance of the flagellate phenotype in populations of *Naegleria* amebae. *Developmental Biology*, *15*, 165–191.

Fulton, C., Webster, C., & Wu, J. S. (1984). Chemically defined media for cultivation of *Naegleria gruberi* (amebae/minimal medium/nutritional requirements). *Proceedings of the National Academy of Sciences*, *81*, 2406–2410.

Garbett, K., Darnall, D. W., Klotz, I. M., & Williams, R. J. P. (1969). Spectroscopy and structure of hemerythrin. *Archives of Biochemistry and Biophysics*, *135*, 419–434.

Gilberthorpe, N. J., Lee, M. E., Stevanin, T. M., Read, R. C., & Poole, R. K. (2007). NsrR: A key regulator circumventing *Salmonella enterica* serovar Typhimurium oxidative and nitrosative stress *in vitro* and in IFN-γ-stimulated J774.2 macrophages. *Microbiology*, *153*(6), 1756–1771.

Gray, M. W., Burger, G., Derelle, R., Klimeš, V., Leger, M. M., Sarrasin, M., Vlček, Č., Roger, A. J., Eliáš, M., & Lang, B. F. (2020). The draft nuclear genome sequence and predicted mitochondrial proteome of *Andalucia godoyi*, a protist with the most gene-rich and bacteria-like mitochondrial genome. *BMC Biology*, *18*(1), 22.

Griffin, J. L. (1972). Temperature tolerance of pathogenic and nonpathogenic free-living amoebas. *Science*, *178*(4063), 869–870.

Hou, S., Larsen, R. W., Boudko, D., Riley, C. W., Karatan, E., Zimmer, M., Ordal, G. W., & Alam, M. (2000). Myoglobin-like aerotaxis transducers in Archaea and Bacteria. *Nature*, *403*, 540–544.

Howard, J. B., & Reest, D. C. (1991). Perspectives on non-heme iron protein chemistry. *Advances in Protein Chemistry*, *42*, 199–280.

Jin, S., Kurtz, D. M., Liu, Z. J., Rose, J., & Wang, B. C. (2002). X-ray crystal structures of reduced rubrerythrin and its azide adduct: A structure-based mechanism for a non-heme diiron peroxidase. *Journal of the American Chemical Society*, *124*(33), 9845–9855.

Jung, S. Y., Kim, J. H., Song, K. J., Lee, Y. J., Kwon, M. H., Kim, K., Park, S., Im, K. il, & Shin, H. J. (2009). Gene silencing of nfa1 affects the in vitro cytotoxicity of *Naegleria fowleri* in murine macrophages. *Molecular and Biochemical Parasitology*, *165*(1), 87–93.

Justino, M. C., Almeida, C. C., Teixeira, M., & Saraiva, L. M. (2007). *Escherichia coli* di-iron YtfE protein is necessary for the repair of stress-damaged iron-sulfur clusters. *Journal of Biological Chemistry*, *282*(14), 10352–10359.

Kao, W. C., Wang, V. C. C., Huang, Y. C., Yu, S. S. F., Chang, T. C., & Chan, S. I. (2008). Isolation, purification and characterization of hemerythrin from *Methylococcus capsulatus* (Bath). *Journal of Inorganic Biochemistry*, *102*(8), 1607–1614.

Klippenstein, G. L. (1980). Structural aspects of hemerythrin and myohemerythrin. *American Zoologist*, *20*(1), 39–51.

Klippenstein, G. L., van Riper, D. A., & Oosterom, E. A. (1972). A comparative study of the oxygen transport proteins of *Dendrostomum pyroides*. *The Journal of Biological Chemistry*, *247*, 5959–5963.

Kurt, D. M., Shriver, D. F., & Klotz, I. M. (1977). Structural chemistry of hemerythrin. *Coordination Chemistry Reviews*, *24*, 145–178.

Liechti, N., Schürch, N., Bruggmann, R., & Wittwer, M. (2018). The genome of *Naegleria lovaniensis*, the basis for a comparative approach to unravel pathogenicity factors of the human pathogenic amoeba *N. fowleri*. *BMC Genomics*, *19*(1).

Liu, Y. J., Han, X. M., Ren, L. L., Yang, H. L., & Zeng, Q. Y. (2013). Functional divergence of the glutathione S-transferase supergene family in physcomitrella patens reveals complex patterns of large gene family evolution in land plants. *Plant Physiology*, *161*(2), 773–786.

Mach, J., Bíla, J., Ženíšková, K., Arbon, D., Malych, R., Glavanakovová, M., Nývltová, E., & Sutak, R. (2018). Iron economy in *Naegleria gruberi* reflects its metabolic flexibility. *International Journal for Parasitology*, *48*(9–10), 719–727.

Maralikova, B., Ali, V., Nakada-Tsukui, K., Nozaki, T., van der Giezen, M., Henze, K., & Tovar, J. (2010). Bacterial-type oxygen detoxification and iron-sulfur cluster assembly in amoebal relict mitochondria. *Cellular Microbiology*, *12*(3), 331–342.

Mastronicola, D., Testa, F., Forte, E., Bordi, E., Pucillo, L. P., Sarti, P., & Giuffrè, A. (2010). Flavohemoglobin and nitric oxide detoxification in the human protozoan parasite *Giardia intestinalis*. *Biochemical and Biophysical Research Communications*, *399*(4), 654–658.

Matthiadis, A., & Long, T. A. (2016). Further insight into BRUTUS domain composition and functionality. *Plant Signaling and Behavior*, *11*(8).

Mustacich, D., & Powis, G. (2000). Thioredoxin reductase. *Biochemical Journal*, *346*, 1–8.

Muto, Y., Nishiyama, M., Nita, A., Moroishi, T., & Nakayama, K. I. (2017). Essential role of FBXL5-mediated cellular iron homeostasis in maintenance of hematopoietic stem cells. *Nature Communications*, *8*.

Nardini, M., Pesce, A., Thijs, L., Saito, J. A., Dewilde, S., Alam, M., Ascenzi, P., Coletta, M., Ciaccio, C., Moens, L., & Bolognesi, M. (2008). Archaeal protoglobin structure indicates new ligand diffusion paths and modulation of haem-reactivity. *EMBO Reports*, *9*(2), 157–163.

Nicoletti, F. P., Comandini, A., Bonamore, A., Boechi, L., Boubeta, F. M., Feis, A., Smulevich, I., & Boffi, A. (2010). Sulfide binding properties of truncated hemoglobins. *Biochemistry*, *49*(10), 2269–2278.

Nývltová, E., Smutná, T., Tachezy, J., & Hrdý, I. (2016). OsmC and incomplete glycine decarboxylase complex mediate reductive detoxification of peroxides in hydrogenosomes of *Trichomonas vaginalis*. *Molecular and Biochemical Parasitology*, *206*(1–2), 29–38.

Onoda, A., Okamoto, Y., Sugimoto, H., Shiro, Y., & Hayashi, T. (2011). Crystal structure and spectroscopic studies of a stable mixed-valent state of the hemerythrin-like domain of a bacterial chemotaxis protein. *Inorganic Chemistry*, *50*(11), 4892–4899.

Opperdoes, F. R., de Jonckheere, J. F., & Tielens, A. G. M. (2011). *Naegleria gruberi* metabolism. *International Journal for Parasitology*, *41*(9), 915–924.

Ouellet, H., Ouellet, Y., Richard, C., Labarre, M., Wittenberg, B., Wittenberg, J., & Guertin, M. (2002). Truncated hemoglobin HbN protects *Mycobacterium bovis* from nitric oxide. *Proceedings of the National Academy of Sciences*, *99*(9), 5902–5907.

Page, F. C. (1967). Taxonomic criteria for limax amoebae, with descriptions of 3 new species of *Hartmannella* and 3 of *Vahlkampfia*. *The Journal of Protozoology*, *14*(3), 499–521.

Parrilli, E., Giuliani, M., Giordano, D., Russo, R., Marino, G., Verde, C., & Tutino, M. L. (2010). The role of a 2-on-2 haemoglobin in oxidative and nitrosative stress resistance of Antarctic *Pseudoalteromonas haloplanktis* TAC125. *Biochimie*, *92*(8), 1003–1009.

Pham, A. N., Xing, G., Miller, C. J., & Waite, T. D. (2013). Fenton-like copper redox chemistry revisited: Hydrogen peroxide and superoxide mediation of copper-catalyzed oxidant production. *Journal of Catalysis*, *301*, 54–64.

Pütz, S., Gelius-Dietrich, G., Piotrowski, M., & Henze, K. (2005). Rubrerythrin and peroxiredoxin: Two novel putative peroxidases in the hydrogenosomes of the microaerophilic protozoon *Trichomonas vaginalis*. *Molecular and Biochemical Parasitology*, *142*(2), 212–223.

Rhee, S. G. (2016). Overview on Peroxiredoxin. *Molecules and Cells*, *39*(1), 1–5.

Roy, A., Kucukural, A., & Zhang, Y. (2010). I-TASSER: A unified platform for automated protein structure and function prediction. *Nature Protocols*, *5*(4), 725–738.

Salahudeen, A. A., Thompson, J. W., Ruiz, J. C., Ma, H. W., Kinch, L. N., Li, Q., Grishin, N. v., & Bruick, R. K. (2009). An E3 ligase possessing an iron-responsive hemerythrin domain is a regulator of iron homeostasis. *Science*, *326*(5953), 722–726.

Santara, S. sen, Roy, J., Mukherjee, S., Bose, M., Saha, R., & Adak, S. (2013). Globin-coupled heme containing oxygen sensor soluble adenylate cyclase in *Leishmania* prevents cell death during hypoxia. *Proceedings of the National Academy of Sciences of the United States of America*, *110*(42), 16790–16795.

Sato, Y., Kameya, M., Fushinobu, S., Wakagi, T., Arai, H., Ishii, M., & Igarashi, Y. (2012). A novel enzymatic system against oxidative stress in the thermophilic hydrogen-oxidizing bacterium *Hydrogenobacter thermophilus*. *PLoS ONE*, *7*(4).

Schardinger, F. (1899). Entwicklungskreis eine *Amoeba lobosa* (Gymnamoeba): *Amoeba Gruberi*. *Sitzungsberichte.*, *108*, 713–734.

Sepasi Tehrani, H., & Moosavi-Movahedi, A. A. (2018). Catalase and its mysteries. *Progress in Biophysics and Molecular Biology*, *140*, 5–12.

Shin, H.-J., Cho, M., Jung, S., Kim, H., Park, S., Kim, H., & Im, K. (2001). Molecular cloning and characterization of a gene encoding a 13.1 kDa antigenic protein of *Naegleria fowleri*. *The Journal of Eukaryotic Microbiology*, *48*(6), 713–717.

Shu, C., Sung, M. W., Stewart, M. D., Igumenova, T. I., Tan, X., & Li, P. (2012). The structural basis of iron sensing by the human F-box protein FBXL5. *ChemBioChem*, *13*(6), 788–791.

Silva, L. S. O., Baptista, J. M., Batley, C., Andrews, S. C., & Saraiva, L. M. (2018). The di-iron RIC protein (YtfE) of *Escherichia coli* interacts with the DNA-binding protein from starved cells (Dps) to diminish RIC protein-mediated redox stress. *Journal of Bacteriology*, *200*(24).

Stairs, C. W., Kokla, A., Ástvaldsson, Á., Jerlström-Hultqvist, J., Svärd, S., & Ettema, T. J. G. (2019). Oxygen induces the expression of invasion and stress response genes in the anaerobic salmon parasite *Spironucleus salmonicida*. *BMC Biology*, *17*(1).

Steven Meshnick, A. R. (1989). *Plasmodium falciparum*: Inhibitor sensitivity of the endogenous superoxide dismutase. *Experimental Parasitology*, *69*, 125–128.

Suzuki, T., Hashimoto, T., Yabu, Y., Kido, Y., Sakamoto, K., Nihei, C. I., Hato, M., Suzuki, S. I., Amano, Y., Nagai, K., Hosokawa, T., Minagawa, N., Ohta, N., & Kita, K. (2004). Direct evidence for cyanide-insensitive quinol oxidase (alternative oxidase) in apicomplexan parasite *Cryptosporidium parvum*: Phylogenetic and therapeutic implications. *Biochemical and Biophysical Research Communications*, *313*(4), 1044–1052.

Sztukowska, M., Bugno, M., Potempa, J., Travis, J., & Kurtz, D. M. J. (2002). Role of rubrerythrin in the oxidative stress response of *Porphyromonas gingivalis*. *Molecular Microbiology*, *44*(2), 479–488.

Thannickal, V. J. (2009). Oxygen in the evolution of complex life and the price we pay. *American Journal of Respiratory Cell and Molecular Biology*, *40*(5), 507–510.

Traverso, M. E., Subramanian, P., Davydov, R., Hoffman, B. M., Stemmler, T. L., & Rosenzweig, A. C. (2010). Identification of a hemerythrin-like domain in a P1B-type transport ATPase. *Biochemistry*, *49*(33), 7060–7068.

Tsaousis, A. D., Nývltová, E., Šuták, R., Hrdý, I., & Tachezy, J. (2014). A Nonmitochondrial hydrogen production in *Naegleria gruberi*. *Genome Biology and Evolution*, *6*(4), 792–799.

Vanlerberghe, G. C. (2013). Alternative oxidase: A mitochondrial respiratory pathway to maintain metabolic and signaling homeostasis during abiotic and biotic stress in plants. *International Journal of Molecular Sciences*, *14*(4), 6805–6847.

Vinogradov, S. N., Bailly, X., Smith, D. R., Tinajero-Trejo, M., Poole, R. K., & Hoogewijs, D. (2013). Microbial eukaryote globins. *Advances in Microbial Physiology*, *63*, 391–446.

Vinogradov, S. N., & Moens, L. (2008). Diversity of globin function: Enzymatic, transport, storage, and sensing. *Journal of Biological Chemistry*, *283*(14), 8773–8777.

Vinogradov, S. N., Tinajero-Trejo, M., Poole, R. K., & Hoogewijs, D. (2013). Bacterial and archaeal globins - A revised perspective. *Biochimica et Biophysica Acta - Proteins and Proteomics*, *1834*(9), 1789–1800.

Vos, M. H., Battistoni, A., Lechauve, C., Marden, M. C., Kiger, L., Desbois, A., Pilet, E., de Rosny, E., & Liebl, U. (2008). Ultrafast heme-residue bond formation in six-coordinate heme proteins: Implications for functional ligand exchange. *Biochemistry*, *47*(21), 5718–5723.

Wakagi, T. (2003). Sulerythrin, the smallest member of the rubrerythrin family, from a strictly aerobic and thermoacidophilic archaeon, *Sulfolobus tokodaii* strain 7. *FEMS Microbiology Letters*, *222*(1), 33–37.

Weber, R. E., & Vinogradov, S. N. (2001). Nonvertebrate hemoglobins: functions and molecular adaptations. *Physiological Reviews*, *81*(2), 569–628.

Weinberg, M. v., Jenney, F. E., Cui, X., & Adams, M. W. W. (2004). Rubrerythrin from the hyperthermophilic archaeon *Pyrococcus furiosus* is a rubredoxin-dependent, iron-containing peroxidase. *Journal of Bacteriology*, *186*(23), 7888–7895.

Wu, Guanghui, Wainwright, L. M., & Poole, R. K. (2003). Microbial Globins. *Advances in Microbial Physiology*, *47*, 255–310.

Wu, Guoyao, Fang, Y.-Z., Yang, S., Lupton, J. R., & Turner, N. D. (2004). Glutathione metabolism and its implications for health. *The Journal of Nutrition*, *134*(3), 489–492.

Xiong, J., Kurtz, D. M., Ai, J., & Sanders-Loehr, J. (2000). A hemerythrin-like domain in a bacterial chemotaxis protein. *Biochemistry*, *39*(17), 5117–5125.

Zielazinski, E. L., González-Guerrero, M., Subramanian, P., Stemmler, T. L., Argüello, J. M., & Rosenzweig, A. C. (2013). *Sinorhizobium meliloti* Nia is a P1B-5-ATPase expressed in the nodule during plant symbiosis and is involved in Ni and Fe transport. *Metallomics*, *5*(12), 1614–1623.